Reactive facies: An approach for parameterizing field-scale reactive transport models using geophysical methods

Douglas S. Sassen,[1] Susan S. Hubbard,[2] Sergio A. Bea,[2,3] Jinsong Chen,[2] Nicolas Spycher,[2] and Miles E. Denham[4]

[1] Developing a predictive understanding of subsurface contaminant plume evolution and natural attenuation capacity is hindered by the inability to tractably characterize controlling reactive transport properties over field-relevant scales. Here we explore a concept of reactive facies, which is based on the hypothesis that subsurface units exist that have unique distributions of properties that influence reactive transport. We further hypothesize that geophysical methods can be used to identify and spatially distribute reactive facies and their associated parameters. We test the reactive facies concept at a U.S. Department of Energy uranium-contaminated groundwater site, where we have analyzed the relationships between laboratory and field (including radar and seismic tomographic) data sets. Our analysis suggests that there are two reactive facies that have unique distributions of mineralogy, texture, hydraulic conductivity, and geophysical attributes. We use these correlations within a Bayesian framework to integrate the dense geophysical data sets with the sparse core-based measurements. This yields high-resolution (0.25 m × 0.25 m) estimates of reactive facies and their associated properties and uncertainties along the 2-D tomographic transects. Comparison with colocated samples shows that the estimated properties fall within 95% uncertainty bounds. To illustrate the value of reactive facies characterization approach, we used the geophysically estimated properties to parameterize reactive transport models, which were then used to simulate migration of an acidic-U plume through the domain. Modeling results suggest that each identified reactive facies exerts a unique control on plume evolution, highlighting the usefulness of the reactive facies concept for spatially distributing properties that control reactive transport over field-relevant scales.

1. Introduction

1.1. Background

[2] Successful prediction of subsurface contaminant plume evolution and assessment of natural attenuation capacity requires the ability to correctly identify controlling reaction and transport properties and to accurately distribute those properties over relevant scales. Properties controlling reactive transport of a contaminant plume include both hydraulic characteristics (such as permeability) and reactive characteristics (such as mineral surface properties, organic matter content, microbial ecology, and dissolved phases). Spatial heterogeneity of these characteristics strongly influences the evolution of a contaminant plume. However, parameterization of this heterogeneity is severely limited by the sparse nature of subsurface sampling using borehole approaches. For example, established hydrological characterization methods (such as pumping, slug and flowmeter tests) are commonly used to measure hydraulic conductivity in the vicinity of the wellbore [e.g., Freeze and Cherry, 1979; Butler, 2005; Molz et al., 1994]; wellbore fluid samples are often used for water quality assessment [e.g., Chapelle, 2001]; and laboratory analysis of retrieved core samples is often used to characterize reactive mineralogy. Unfortunately, data obtained from borehole methods is typically sparse relative to the simulation volume and thus may not capture sufficient information away from the wellbore to describe the key controls on subsurface flow or reactions. The inability to characterize controlling properties at a high enough spatial resolution and over a large enough volume often hinders our ability to accurately simulate subsurface flow and transport processes. To circumvent this common obstacle, we explore if properties that control reactive transport can be associated with a subsurface unit that is discernible with geophysical methods in order to both

[1]Earth Sciences Division, Lawrence Berkeley National Laboratory, Berkeley, California, USA.
[2]Lawrence Berkeley National Laboratory, Berkeley, California, USA.
[3]Now at CONICET-IHLLA, Azul, Argentina.
[4]Environmental Science and Biotechnology, Savannah River National Laboratory, Aiken, South Carolina, USA.

Corresponding author: S. S. Hubbard, Lawrence Berkeley National Laboratory, 1 Cyclotron Rd., Mail Stop 90R1116, Berkeley, CA 94720-8126, USA. (sshubbard@lbl.gov)

.

simplify the task of characterizing heterogeneous systems and to ameliorate the problem of inadequate sampling. Moreover, we explore the potential of geophysical methods for identifying and spatially distributing these reactive facies over field scales, as is needed to improve predictions of subsurface contaminant transport.

[3] The reactive facies concept is based on the hypotheses that subsurface units can be identified, which have shared properties that influence flow and reactive transport that are distinct from surrounding units. A facies is an assemblage of like characteristics, usually reflecting the origin of a rock unit that serves to differentiate the unit from neighboring or related rock units [*Koltermann and Gorelick*, 1996]. Some common facies types include lithofacies (defined on the basis of petrographic properties); sedimentary/depositional facies (defined by geologic origins [*Reading and Lovell*, 1996; *Anderton*, 1985]), and hydrofacies (sediment units that share distinctive hydraulic properties used for parameterizing hydrology models); [*Poeter and Gaylord*, 1990; *Klingbeil et al.*, 1999, *Heinz et al.*, 2003; *Zappa et al.*, 2006]. One of the main advantages of facies-based approaches is that they can significantly simplify the task of characterizing complex heterogeneous systems by subdividing the subsurface into a finite number of relatively homogeneous units that can be more easily described and characterized.

[4] Evidence suggests that facies-based approaches often better represent subsurface property distributions compared to distributions obtained from interpolation of point measurements [*Fogg et al.*, 1998; *Falivene et al.*, 2006; *Michael et al.*, 2010; *Zappa et al.*, 2006]. Hydrofacies-based approaches for characterizing hydrologic properties can often better represent sharp contrasts observed between different deposits and better represent the interconnectivity of conductive bodies relative to traditional interpolation techniques that spatially smooth heterogeneities [e.g., *de Marsily et al.*, 2005]. *Eggleston and Rojstaczar* [1998] showed that hydrofacies, identified through wellbore sampling and used as input to flow and transport models, improved the estimated distribution of a contaminant plume compared to other methods used to develop the model domain parameters (such as kriging and polynomial regression).

[5] The use of facies to characterize contaminant reactivity in highly heterogeneous environments has also shown significant promise. *Kleineidam et al.* [1999] showed that the sorption of hydrophobic organic contaminants in a fluvial aquifer depends on the source, petrographic composition, and depositional processes of the sediment. They observed increased rates of sorption and higher proportions of organic sediment grains in gravel-dominated facies when compared to sand-dominated facies. These variations were traced to differences in source rock (organic rich sedimentary rocks versus silicate dominated igneous and metamorphic rocks) and to differences in sediment maturity (highly transported and weathered sands compared to gravels). The study of *Kleineidam et al.* [1999] emphasized the importance of not only differences in lithofacies, but also the history and source of the sediments that constitute a facies. *van Helvoort et al.* [2005] studied the reactive potential of different sediments within an unconfined fluvial aquifer and found improved predictive ability when sediment samples were subdivided into sedimentary facies. They showed that accounting for postdepositional facies-based processes (such as facies-selective oxidation or reduction of mineral and organic components) led to improved prediction of groundwater reactivity over models that disregarded postdepositional alterations. These studies suggest that by using a facies based approach along with careful laboratory analysis, reactive behavior can be better characterized.

[6] Although attempts have been made to link subsurface units with hydrogeological or reactive properties, only a few studies have explored the link of facies with both of these properties together. *Scheibe et al.* [2006] conducted numerical studies to explore the impact of coupled physiochemical properties (including clay content, hydraulic conductivity, and iron sediment geochemistry) on the efficacy of uranium bioremediation. In their synthetic study, they used subsurface hydraulic conductivity and geophysically obtained Fe(III) estimates from the U.S. Department of Energy (DOE) South Oyster Bacterial Transport Site [*Hubbard et al.*, 2001; *Chen et al.*, 2004] and assumed a negative correlation between the hydrological and sediment geochemical properties. *Li et al.* [2010] also performed numerical studies to explore the impact of coupled physiochemical properties on uranium transport associated with the DOE Integrated Field Research Center in Rifle, CO. They found that linked hydraulic conductivity and Fe(III) distributions resulted in localized larger accumulation of remediation-induced biomass and precipitates relative to homogeneous or independent heterogeneities, which led to a greater possibility of pore clogging. *Allen-King et al.* [1998] categorized relatively homogeneous core samples on the basis of sediment facies in the Borden Aquifer and found good correlations between hydraulic conductivity (K) and adsorption coefficient (Kd) when the data were subdivided by facies [*Allen-King et al.*, 1998]. Together, these studies suggest that a reactive facies based approach may provide a simple, yet effective, framework for describing coupled physiochemical properties that govern subsurface flow and transport.

[7] Herein, we explore if reactive facies can be identified, distributed over field scales using geophysical data, and used to parameterize reactive transport models. In the last decade, geophysical methods have been used extensively for shallow subsurface mapping, parameter estimation, and process monitoring [e.g., *Rubin and Hubbard*, 2005; *Vereecken et al.*, 2006]. The main advantage of using geophysical data to complement conventional measurements is that geophysical methods can provide spatially extensive information about the subsurface in a minimally invasive manner at a comparatively high resolution. The greatest disadvantage is that the geophysical methods only provide indirect proxy information about subsurface properties or processes: petrophysical models and integration methods are commonly used to extract quantitative estimates of subsurface flow and transport properties from the geophysical data [e.g., *Hubbard and Linde*, 2010; *Slater*, 2007].

[8] Petrophysical relationships are often developed through comparison of geophysical attributes at wellbore locations with measurements made in the wellbore or using wellbore-derived core. The comparison of geophysical and single "point" measurements suffers from two main drawbacks. The first complication stems from the differences in measurement support volume of geophysical measurements and the direct measurements [e.g., *Ferré et al.*, 2005; *Moysey et al.*, 2005; *Day-Lewis et al.*, 2005]. The support

scale of geophysical measurements is related to the resolution of the method (which in turn is governed by factors such as acquisition method, geometry, and material properties); it is generally much larger than the support scale of direct measurements. In addition to scale-matching problems, wellbore drilling and laboratory analysis of individual core samples (which are used to assess permeability, porosity, sorting, and mineralogy) often disturb the material, rendering the measurements less representative of the in situ conditions that are sampled by the geophysical signals. Statistical development of petrophysical relationships between physiochemical properties and geophysical attributes requires a large number of analyzed samples. Because reactive facies are likely to be larger than the geophysical measurement support scale, a reactive facies based characterization approach has the potential to minimize the scale-matching problem and increase the statistical significance of the petrophysical relationship.

[9] Many geophysical attributes have the potential to be sensitive to facies-based architecture and associated parameter suites. Indeed, the juxtaposition of different facies and the resulting seismic signature of the interface led to the development of a concept called seismic facies [*Sangree and Widmier*, 1979], which has been widely used to delineate stratigraphic architecture for the exploration of hydrocarbons. The concept of using geophysical methods to delineate the architecture of sedimentary units has been adopted for the shallower subsurface using many different geophysical methods, including seismic, electrical [*Gerilynn et al.*, 1995], and ground-penetrating radar (GPR) [*Neal*, 2004; *van Overmeeren*, 1998].

[10] Related to the facies concept, many studies have illustrated the value of geophysical methods for characterizing aquifer zonation, and in turn, for improving the understanding of subsurface flow and transport. *Hyndman and Gorelick* [1996] used seismic tomographic travel time data in conjunction with slug and tracer data to identify zones within an aquifer that had similar hydraulic properties. *Tronicke et al.* [2004] utilized both GPR travel time and attenuation tomography to delineate aquifer zones using multivariate statistics. *Paasche et al.* [2006] utilized a clustering technique to define aquifer zones based on the response of multiple geophysical techniques and hydrological measurements. *Linde et al.* [2006] developed a methodology for inverting tracer test data using zonation information obtained from two-dimensional radar tomograms to improve the (typically overly smooth) hydraulic conductivity fields obtained from conventional inversion of tracer test data. The method simultaneously yielded two-dimensional estimates of hydraulic conductivity as well as petrophysical relationships that relate hydraulic conductivity to radar velocity for each key zone. *Chen et al.* [2004] utilized a Bayesian methodology and observed correlations between mud content and GPR attenuation to quantify the distribution of lithofacies in a shallow, unconfined aquifer. *Hubbard et al.* [2008] used cross-hole radar and seismic measurements with wellbore flowmeter data and a statistical approach to identify hydraulic zonation within a Cr(VI) contaminated aquifer at the DOE Hanford Site in Washington. They found that the hydrological zonation greatly controlled the distribution of amendments that were injected into the subsurface to stimulate bioremediation as well as the location of the induced biogeochemical transformations. *Chen et al.* [2010] jointly inverted surface seismic refraction travel time and wellbore-based lithological information to delineate subsurface zonation at the contaminated Oak Ridge National Laboratory. They used the results to identify the presence of a narrow and laterally extensive subsurface feature that was interpreted to control plume transport.

[11] A common hypothesis for many of these studies is that the geophysical attribute (such as electrical conductivity, GPR attenuation, or seismic velocity) is sensitive to the bulk or effective soil properties (such as composition, texture, grain size, or sorting) associated with facies. A secondary hypothesis, explored by *Chen et al.* [2004], is that the sensitivity of geophysical attributes to lithofacies could also be used to quantify sediment geochemistry through exploiting the mutual dependence of geophysical attributes and sediment geochemistry on lithology. Using cross-hole tomographic GPR data collected in conjunction with wellbore core sediment extract data, *Chen et al.* [2004] developed and exploited a petrophysical relationship between mud content, iron mineralogy, and GPR attenuation to estimate the spatial distribution of Fe(II) and Fe(III) within a shallow aquifer. Together, these studies suggest that geophysical methods hold significant potential for identifying subsurface units that have distinct distributions of hydrological and geochemical properties.

1.2. Reactive Facies Approach

[12] Previous studies have suggested the value of a facies concept and the potential of geophysical methods to identify facies. Our approach builds on these previous studies to first define the key controls over reactive transport at a particular site, determine if reactive facies exists, and then to determine if geophysical methods can be used to identify and spatially distribute reactive facies and associated properties over field scales as is needed to parameterize reactive transport models. Our approach is schematically indicated in Figure 1. Laboratory-scale analysis is performed to identify the key controls on contaminant reactivity (such as sorption, ion exchange and oxidation) and to determine if these controls are dependent on properties such as mineralogy and texture that may define a reactive facies. In parallel, geophysical analysis and data mining are performed to determine if sediment packages have unique and linked distributions of reactive transport properties, and whether geophysical attributes are able to distinguish the identified reactive facies. If both lines of investigations are successful, then estimation approaches can be used with geophysical data sets to spatially distribute the reactive facies at the field scale.

[13] We develop and test the concept at an acidic, radionuclide-contaminated aquifer located under seepage basins at the F-Area of the U.S. Department of Energy Savannah River Site (SRS), South Carolina. Developing a predictive understanding of long-term plume mobility in the presence of significant pH gradients is important for ascertaining the long-term natural attenuation capacity at this site [*Denham and Vangelas*, 2009; *Dong et al.*, 2012; *Spycher et al.*, 2011]. Advanced laboratory exploration of facies-based surface complexation models, as well as reactive transport model sensitivity analysis studies, associated with this site are ongoing.

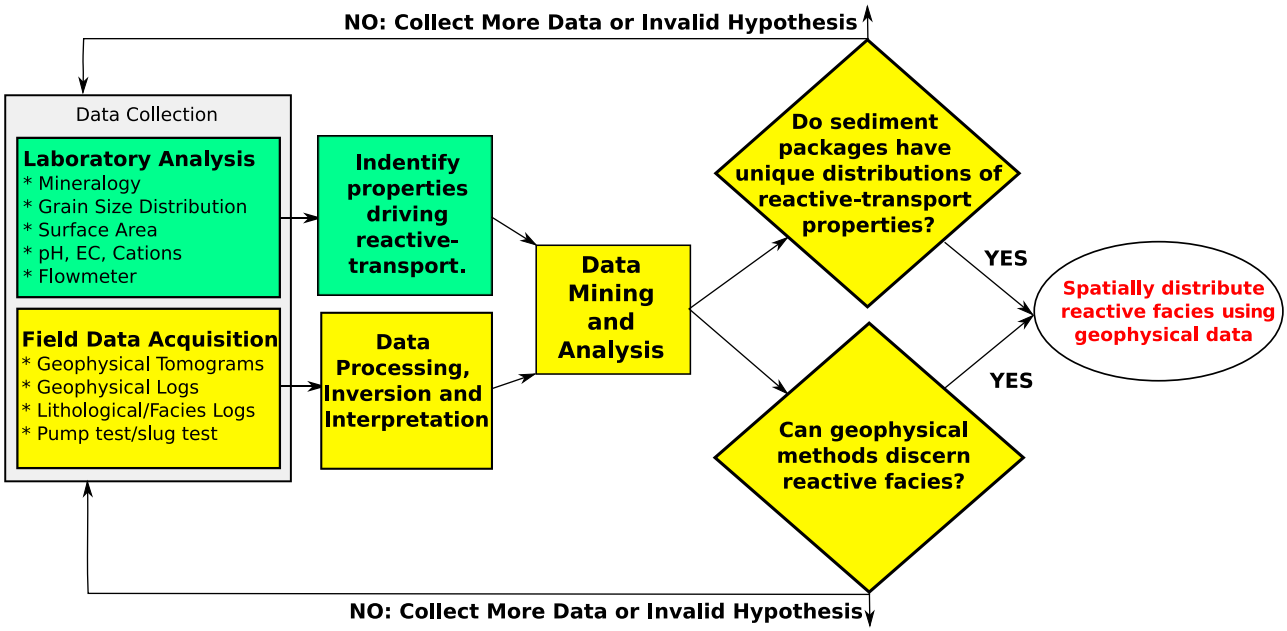

Figure 1. Schematic approach for identifying and distributing reactive facies using laboratory analysis, geophysical methods, and data mining.

[14] Our study is organized as follows. Section 2 provides a description of the study site and the geochemical, geophysical, geological, and hydrological data sets collected at the site. The methodology used to integrate these various data in the identification and estimation of reactive facies is described in section 3. Results and conclusions are provided in section 4.

2. Study Site, Data Sets, and Methodology

2.1. The Savannah River Site: F-Area Seepage Basins

[15] The SRS is located approximately 160 km from the Atlantic Coast and is underlain by poorly consolidated Atlantic Coastal Plain sediments. The SRS covers an almost circular area of about 800 square kilometers and contains facilities constructed in the early 1950s to produce plutonium and tritium for the U.S. nuclear weapons stockpile. SRS has approximately 172×10^6 m^3 of groundwater, soil, and debris contaminated with metals, radionuclides, and organics [*NRC*, 2000] as a result of on-site disposal practices. The SRS F-Area Seepage Basins are located in the north central portion of SRS and consist of three unlined, earthen surface impoundments that received approximately 1.8 billion gallons (7.1 billion liters) of acidic, low-level waste solutions. The acidic liquid waste (average influent pH of 2.9) originated from the processing of irradiated uranium in the F-Area Separations facility from 1950 through 1989. As a result, the sediments that underlie the F-Area have been exposed to acidic solutions for many decades. The groundwater is currently acidic, with pH values as low as 3.2 near the basins. The plume currently extends from the basins approximately 600 m down gradient to a receiving stream, and contains a large number of contaminants. Based on risk to potential receptors, the most hazardous contaminants are uranium isotopes, Sr-90, I-129, Tc-99, tritium, and nitrate. The basins were closed and capped in 1991. A pump-and-treat remediation system began operation in 1997, and it was replaced in 2004 by a hybrid funnel-and-gate system installed about 300 m up gradient from the stream (see Figure 2). Alkaline solutions are now being injected into the subsurface near the gates in an attempt to neutralize the acidic groundwater down gradient of the seepage basins. Monitored Natural Attenuation (MNA) is the eventual desired closure strategy for the site, based on the conceptual model that rainwater will eventually neutralize the lingering mineral surface acidity, causing an increase in pH, which will lead to sorption of U and thus natural immobilization in the trailing end of the plume. If the natural pH neutralization up gradient from the treatment system is insufficient, additional enhanced neutralization will be required. The development of an understanding of the long-term H^+ and U sorption behavior at the site in the presence of natural heterogeneity is critical to assessing the in situ treatment requirements over the long time frame [*Denham and Vangelas*, 2009; *Wan et al.*, 2012].

[16] Sediments at the site were deposited primarily in shallow marine and fluvial environments [*Gohn*, 1988; *Jean et al.*, 2004]. The site hydrogeology has been described in detail in many site reports [e.g., *Looney et al.*, 1972; *Killian et al.*, 1986; *Strom and Kaback*, 1992]. The contaminant plume related to the F-Area basin (Figure 2) is found within the Upper and Lower Upper Three Rivers Aquifers (UUTRA and LUTRA); these two aquifers are separated by a clay lagoonal deposit [*Jean et al.*, 2004] known as the Tan Clay Confining Zone (TCCZ). The LUTRA is underlain by the Gordon aquitard. The greatest proportion of nitrate and uranium contamination is found in the UUTRA, which is the focus of this study. The UUTRA aquifer is composed of two major depositional facies: barrier beach deposits (which are composed mostly of clean sands), and lagoonal deposits (which are composed of sandy clay) [*Jean et al.*, 2004]. Major minerals identified at the site are quartz (SiO_2),

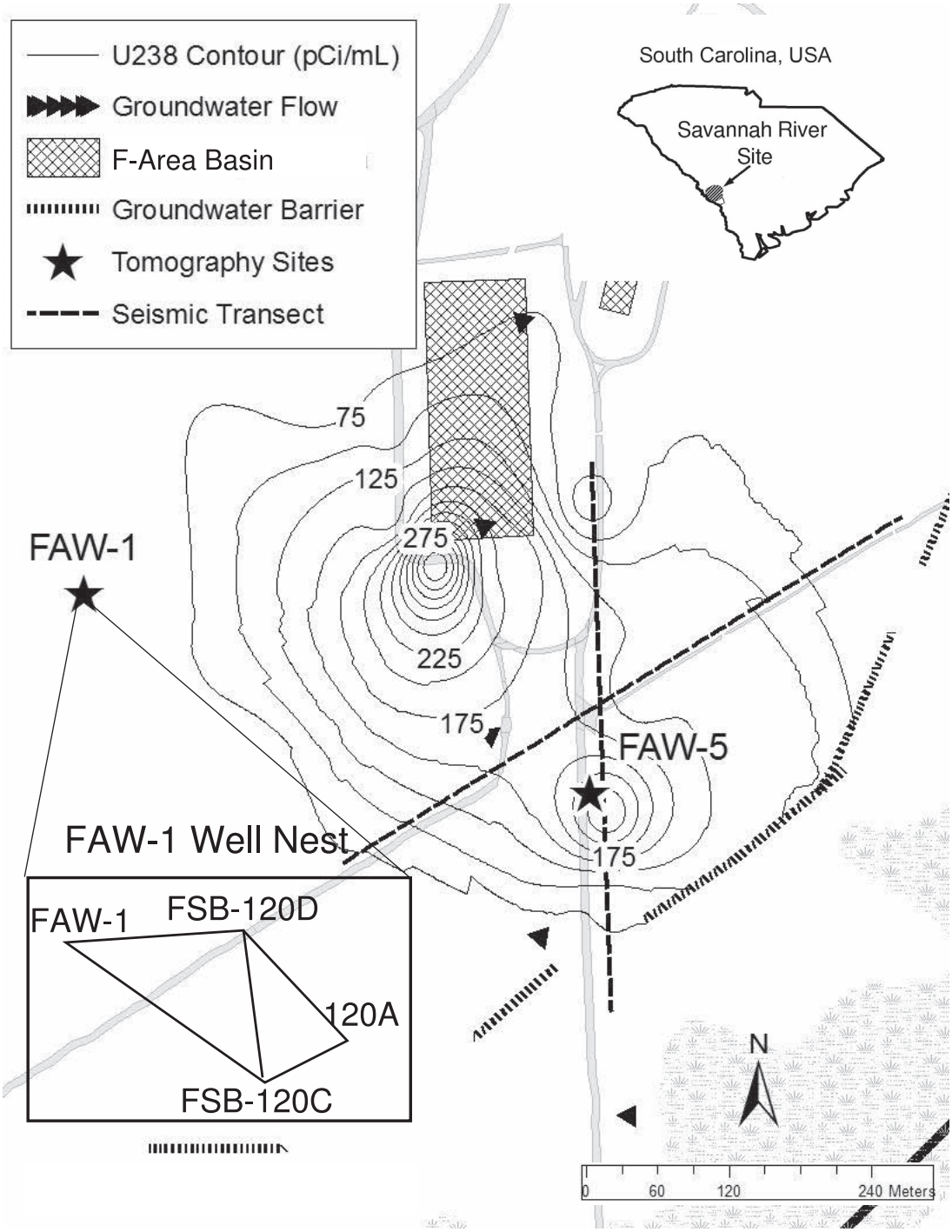

Figure 2. Map of F-Area showing new sampling wells and ^{238}U concentrations. The FAW-1 and FAW-5 wells are located in the local-scale study sites. We focus here on the wellbore and cross-hole data collected at the FAW-1 "clean" local-scale study site.

kaolinite ($Al_2Si_2O_5OH_4$) and goethite (FeOOH); amounts of other clays and carbonates are typically negligible in the water table aquifer but increase in deeper aquifers [e.g., *Strom and Kaback*, 1992; *Serkiz et al.*, 2007].

[17] A drilling and sampling campaign was conducted at the F-Area in 2008 at two "local-scale" study sites (Figure 2). One site was developed near wellbore FAW1, which is at the edge of the U plume and is designated the "clean" site for this study. The other site was developed in the heart of the plume near FAW5 and is designated the "contaminated" site. Three other wellbores were drilled throughout the F-Area to provide additional information about the physiochemical properties of the site. All wellbores were drilled through the UUTRA to near the top of the TCCZ and completed with PVC casing. Although deeper drilling would have allowed sampling of the LUTRA (and thus testing the reactive facies

concept over a larger and more geologically variable depth section), concerns about drilling through the TCCZ aquitard dictated the total drilling depth. A total of 34 core samples were retrieved for analysis; analysis of these cores is described in section 2.2. Cross-hole geophysical data sets were collected between wellbores at both of the local-scale study sites, as is also described in section 2.2.

[18] Our goal at this site was to explore, through coupled laboratory and field studies, if the reactive facies concept is viable and if geophysical methods can be used to extrapolate reactive facies at the local scale. In 2010, wellbore logging was performed in all of the wellbores drilled in 2008, and surface seismic data were collected along two transects that were oriented parallel and approximately perpendicular to the plume gradient.

2.2. Data Acquisition and Analysis

2.2.1. Laboratory Analysis

[19] Laboratory analyses of 34 retrieved sediment samples from 5 wells (Figure 2) were performed by *Dong et al.* [2012] and *Seaman et al.* [2009] to gain an understanding of the mineralogical controls on pH-dependent U sorption at the F-Area. Sediment texture was measured using standard hydrometer analysis. The mineralogy was estimated with a combination of X-ray diffraction (XRD) and scanning electron microscopy (SEM) to establish the mineral components and X-ray fluorescence (XRF) to establish the proportion of each mineral. Textural information on samples was found through a combination of sieve and hydrometer analysis. The fine content within our samples varied between 2% and 37%. The surface areas of each sample were estimated by BET analysis.

[20] These recent laboratory investigations were conducted to characterize and explore controlling reactive properties in UUTRA sediments. Major minerals, identified from XRD and SEM images, were quartz, kaolinite and goethite. Because the driving mechanism of uranium sequestration at the site is the pH-dependent sorption of U to kaolinite and goethite [*Dong et al.*, 2012; *Serkiz et al.*, 2007], the abundance and spatial distribution of these minerals are believed to be key sediment properties affecting U transport. Therefore, the volumetric proportions of kaolinite ($Al_2Si_2O_5OH_4$) and goethite (FeOOH), as inferred from measured (XRF) Al:Fe ratios, fine content, and porosity, are likely to be critical for understanding reactive transport at the field scale, and is considered as a key target for the reactive facies characterization effort. Because pH plays an important role in U adsorption, sediment titration experiments were performed to quantify the surface protonation/deprotonation characteristics of F-Area sediments. These experiments consist of first titrating the sediments with an acid down to pH $\sim$3, then titrating the resulting mixture and its supernatant with a base to pH above 9 [after *Ge and Hendershot*, 2004], and recording the amount of base added after each pH reading.

2.2.2. Historical Data Sets

[21] Extensive subsurface core samples and groundwater monitoring data have been collected and summarized in DOE reports over several previous decades. Geologically interpreted descriptive well logs, with information on sediment texture, architecture, and depositional facies [*Smits et al.*, 1997] provide important insights into the distribution of sediments and facies within the contaminated area. These geologic logs show that the UUTRA is dominantly a sand deposit with the percent fines varying between 0 to 40%, as determined though optical counts [*Smits et al.*, 1997]. Accompanying the sediment descriptions are qualitative estimates of porosity from binocular microscope analysis [*Smits et al.*, 1997] and hydraulic conductivity estimates derived from pumping tests [*Denham*, 1999], slug tests and laboratory experiments [*Hamm et al.*, 1996]. The laboratory measurements of hydraulic conductivity within the UUTRA show a range between 1×10^{-1} to 1×10^{-9} cm s^{-1}. The mean hydraulic conductivity of the UUTRA, obtained using pumping tests, is estimated at 3.5×10^{-3} cm s^{-1}. This variability is consistent with previous findings that measurements of hydraulic conductivity are dependent on the measurement support scale [e.g., *Tidwell et al.*, 1999; *Beckie and Harvey*, 2002]; the laboratory measurements have a support scale on the order of tens of cm^3, while the slug tests have a support scale of approximately a few m^3 and pumping tests have support scales on tens of m^3. We derived the hydraulic conductivity distributions as a function of depositional facies by cross-referencing the database of geologic log descriptions along with the database of laboratory-derived hydraulic conductivity values. The UUTRA conductivity values from the laboratory data set show a marked contrast in hydraulic conductivity between the lagoonal and beach/barrier facies.

2.2.3. Geophysical Data

[22] As part of this study, tomographic radar and seismic data were collected between the boreholes at both local scale study sites using both zero offset profiles (ZOP) and multiple offset profiles (MOP) following *Peterson* [2001]. Both seismic and GPR [e.g., *Sangree and Widmier*, 1979] and GPR [e.g., *Neal*, 2004; *van Overmeeren*, 1998] methods have been shown to be useful in distinguishing facies and aquifer zonation, as was described in section 1.1. Also, these methods where chosen because of their relatively high resolution, which is important at the scale of our study. Cross-hole electrical data sets were not acquired because well screens, which are needed for electrolytic conduction, were limited in length and were positioned at various depth intervals in the different wells to meet regulatory sampling requirements. The radar tomographic data were collected using a PulseEKKO 100 system, with 100 MHz central frequency antennas and a transmitter receiver sample interval in the wellbores of 0.25 m. Radar data were collected between depths of 18.5 to 38 m depending on the completion depth of the wells. Radar travel time and amplitude picking, preinversion quality control steps, and inversion procedures were performed following the procedure of *Peterson* [2001]. The first-arrival travel times for all raypath propagating in the saturated zone were picked for each transmitter/receiver location, and an associated amplitude value was calculated as the square root of the sum of the squared amplitude values for all samples within approximately the first 15 nanoseconds following the first break pick. The baseline radar travel times and amplitudes were inverted for radar velocity and attenuation, respectively, using a straight-ray wave algebraic reconstruction technique [*Peterson et al.*, 1985] and a discretization of 0.25 m by 0.25 m. The straight-ray approach is often used when inverting data sets in which radar velocity contrasts are less than $\sim$20% [*Peterson*, 2001]. No wellbore constraints, smoothing, or assumptions about

anisotropy were imposed during the tomographic data inversion process. Source and receiver corrections were performed, however, which attempt to dampen geophysical responses at the borehole caused by disturbances such as washouts or sloughing. Radar signal quality was good through the sandy and sandy clay sections but poor to completely attenuated through the more clay-rich or highly contaminated sections. The GPR attenuation and velocity tomograms particularly show significant amounts of detail between the wellbores. Examples of inverted 2-D radar velocity and attenuation tomograms are shown in Figure 3. Seismic data were collected in the saturated section only, using a Geometrics Geode seismic system, an LBNL piezoelectric source, and an ITI hydrophone sensor string. The central frequency of the pulse was 4000 Hz with a bandwidth from approximately 1000 to 7000 Hz. The source and geophone spacing in the wellbores was 0.25 m. Travel times were picked for all source-receiver pairs and inverted using a 0.25 m by 0.25 m discretization. A straight-ray algebraic reconstruction technique [*Peterson et al.*, 1985] was used to invert the seismic travel time information into estimates of seismic velocity along the 2-D transects and with a 0.25 m by 0.25 m discretization. An example of the 2-D variation in seismic velocity obtained through inversion is shown in Figure 3.

[23] Electrical induction and natural gamma downhole logs were acquired within well nests near the new FAW-1 and FAW-5 wells (Figure 2) as well as within several older wells distributed throughout the F-Area. These logs were acquired with a Mt Sopris system using centimeter scale sampling intervals. These logs where filtered using a moving average window of 0.25 m to remove high-frequency noise and to provide a consistent scale for comparison with the tomographic data. Electrical induction logs are sensitive to pore water conductivity, mineralogy and sediment texture, while natural gamma logs are sensitive to the amount of radioactive elements present and are an indicator of clay content. In wells where depositional facies interpretations of cores were not available, we relied on electric induction and natural gamma logs to provide estimates of

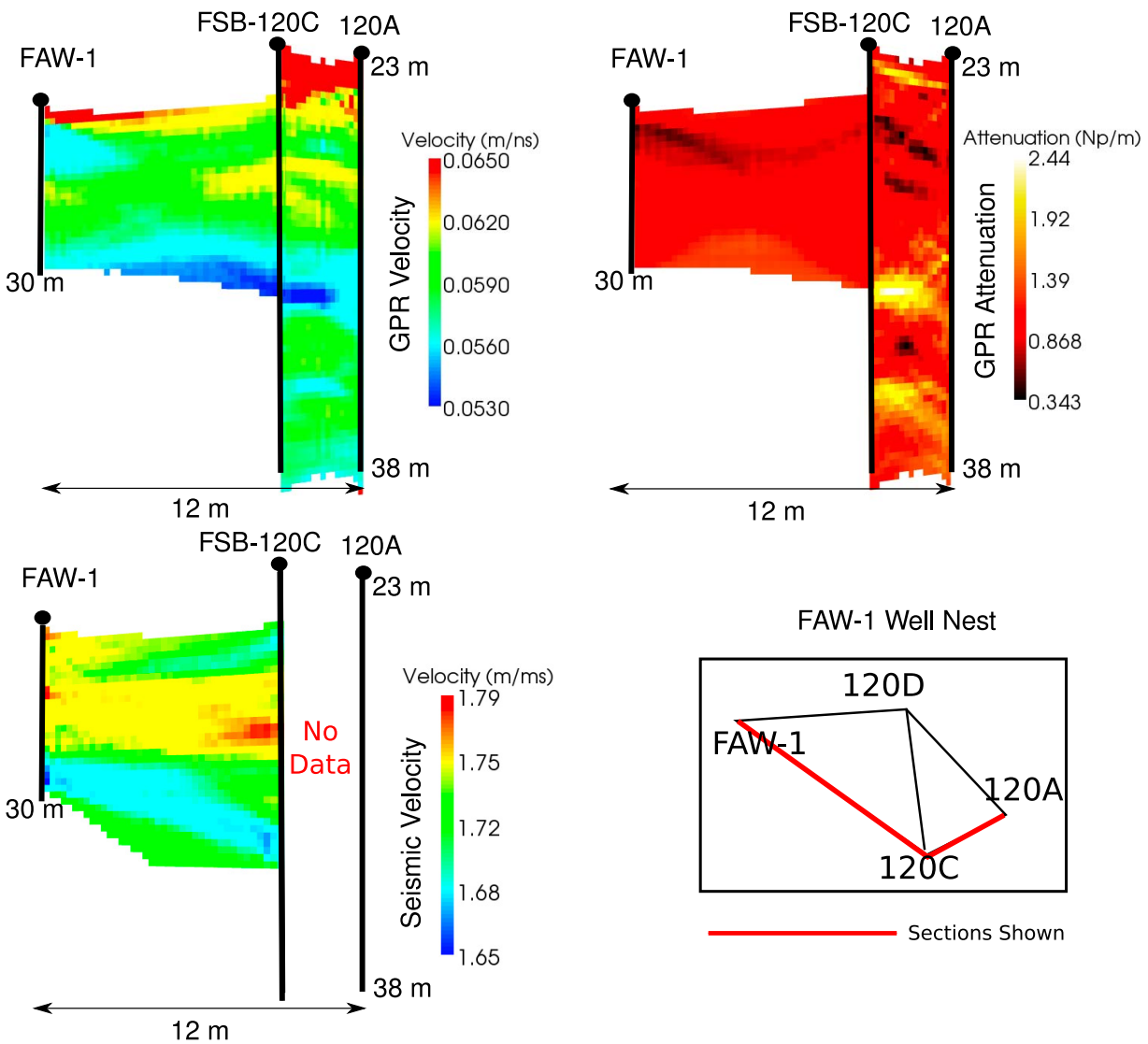

Figure 3. Inverted tomograms of seismic velocity, GPR velocity, and GPR attenuation along 2-D transects in the FAW-1 well nest.

depositional facies. Prior to comparison of the log data and depositional facies interpretations, the geophysical logs where truncated to only include the saturated zone of the UUTRA, and then centered by their mean values and normalized by their standard deviations. This normalization removes bias that may exist between the different logs due to varying wellbore conditions. To consistently interpret depositional facies, we utilized logistical regression [e.g., *Ott and Longnecker*, 2001] on log-based geophysical attributes and depositional facies-based indicator values. We utilized the stepwise deletion model selection procedure for the regression where we started with high-order polynomial equations with all available geophysical attributes. Polynomial terms and/or geophysical attributes not found to contribute to the estimation of depositional facies were dropped from the regression. The logistic regression model has good fit, with a residual deviance of 90.528 on 196 degrees of freedom, where a good fit is interpreted when the degrees of freedom exceed residual deviance. The logistical regression provided the probability of the depositional facies given the geophysical log data (Figure 4).

[24] As an example of the different types of geophysical, lithological, and depositional data available, Figure 5 shows a comparison of a subset of the data near one particular well in the "clean" FAW-l local scale study site, including GPR attenuation and velocity (extracted from the tomogram near the wellbore location), seismic velocity (extracted from the tomogram near the wellbore location), electrical conductivity and gamma values (from wellbore logs), percent mud content and facies interpretation (from historical data sets).

2.3. Methodology

[25] Following the approach illustrated in Figure 1, we first explore if reactive facies exist at the F-Area through statistical analysis of new laboratory data and existing physiochemical properties. Subsequently, analysis is performed to determine if geophysical attributes can identify and distinguish between different reactive facies. If both lines of investigation are successful, then estimation approaches can be used with tomographic data sets to spatially distribute the reactive facies along 2-D transects at the field scale.

2.3.1. Statistical Analysis

[26] Statistical analysis was performed to discover (1) what physical or geochemical property, or combination of properties, control the reactive behavior of uranium at the site and thus define the reactive facies and (2) what geophysical attributes are sensitive to those reactive facies. The data mining focused on a large range of physical, geochemical, and geophysical attributes, including: pH, Kd, hydraulic conductivity (K), XRF elemental analysis, sample color, percent fines, percent sand, percent gravel, depositional facies, sample electrical conductivity, seismic velocity, GPR

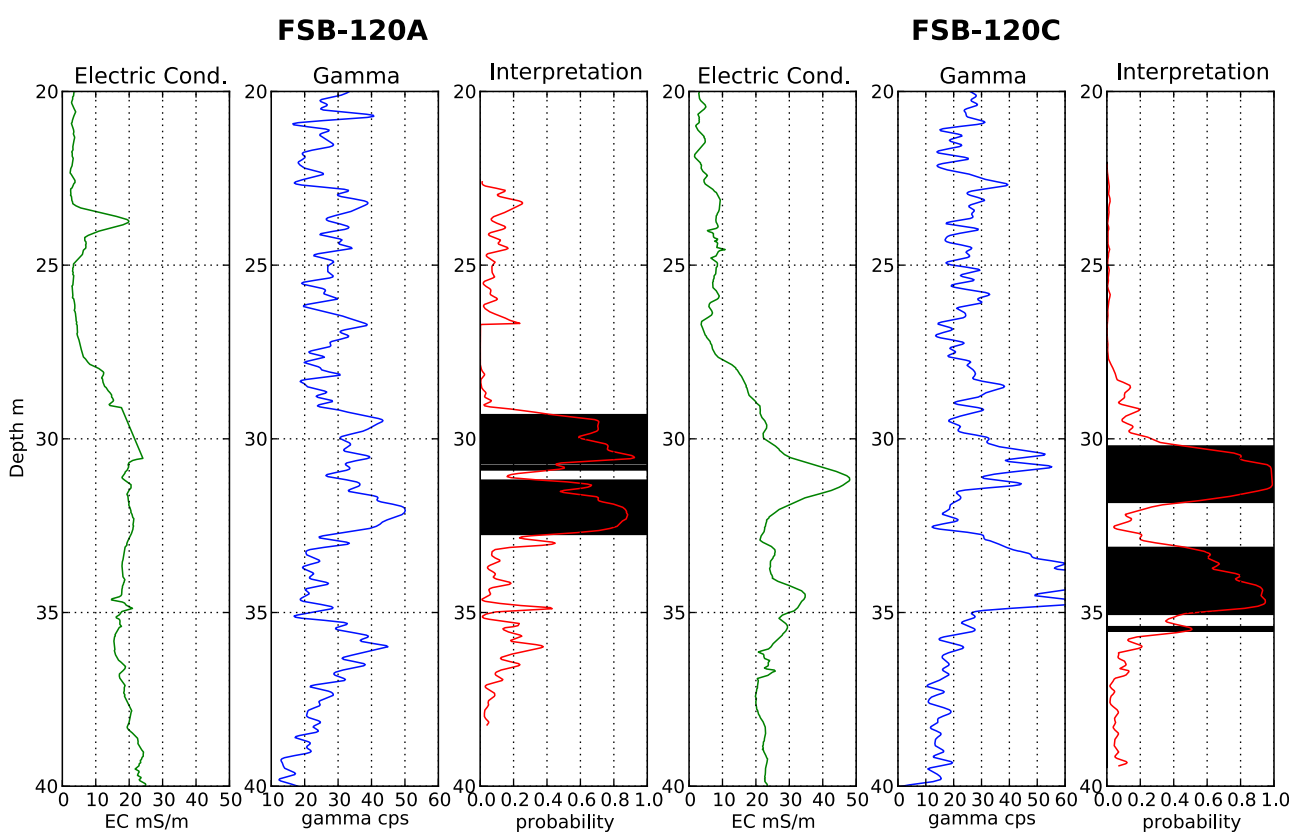

Figure 4. Well logs of electrical conductivity (EC) and natural gamma along with the interpreted depositional facies probability from logistical regression for wells (left) 120A and (right) 120C in the FAW-l well cluster. The red lines on the interpretation plots represent the probability of being in the lagoonal facies, black rectangles represent areas where the probability lagoonal facies exceeded 0.5, and white area indicate the probability of the beach facies exceeds 0.5.

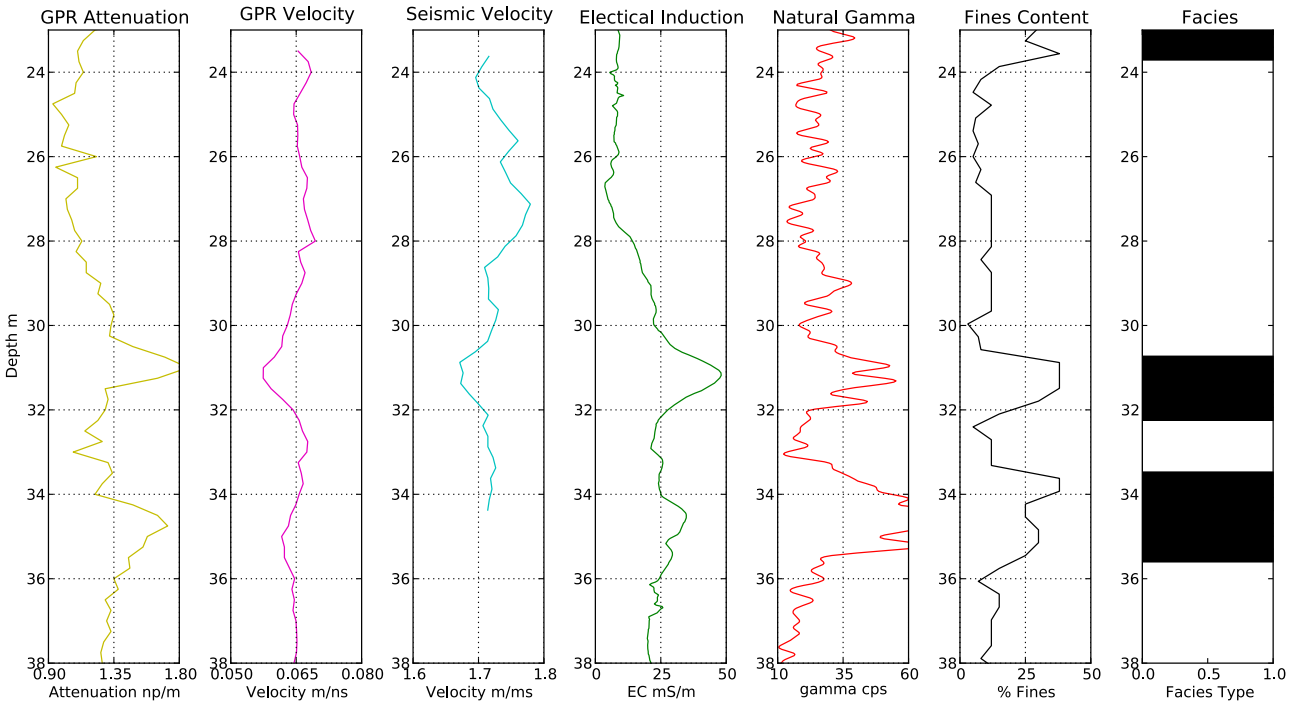

Figure 5. Comparison of geophysical attribute obtained at FSB-120C well using tomographic approaches with sediment texture and depositional facies type at the FSB-120AR well, which is located 1.5 m away, obtained from well logs and core analysis. EC = electrical conductivity.

velocity, and GPR attenuation. Analysis approaches included: unsupervised clustering with a self-organizing maps (SOM), construction of correlation matrices, simple linear and multivariate regression, and descriptive statistics. The self-organizing map was developed using the SOM_PAK software package [*Kohonen et al.*, 1996], and all other statistical analysis was performed using the R statistical package [*R Development Core Team*, 2010].

2.3.2. Bayesian Estimation Approach

[27] A Bayesian framework was developed to incorporate point measurements, geophysical data, and developed petrophysical relationships in the spatial distribution of reactive facies at the F-Area, together with their associated properties and uncertainties. Specifically, we used the Bayesian estimation framework based on the normal linear regression model [*Chen et al.*, 2001]. A Bayesian estimation framework updates a prior probability of reactive facies with, in this case, the tomographic images, to estimate the posterior probability of encountering the reactive facies. The posterior estimate of the reactive facies (F) as a function of GPR attenuation (A), GPR velocity (G), and seismic velocity (S) is given by,

$$p(F|A,G,S) = N \cdot L(G|F,A,S) \cdot L(A|F,S) \cdot L(S|F) \cdot p(F), \quad (1)$$

where N is normalization factor, $L(G|F,S,A)$ is the likelihood function describing the probability of the measured GPR velocity given facies information, seismic velocity and GPR attenuation; $L(A|F,S)$ is the likelihood function describing the probability of the measured GPR attenuation given the facies information and seismic velocity; $L(S|F)$ is the likelihood function describing the probability of the measured seismic velocity given the reactive facies. The last term, $p(F)$, represents the prior probability density function of the reactive facies.

[28] The prior distributions were obtained through kriging wellbore-based data using GSLIB [*Deutsch and Journel*, 1998] using variogram models constructed through analysis of vertically distributed wellbore data and using an assumption of a 3:1 horizontal to vertical anisotropy ratio. Unlike the original example of the *Chen et al.* [2001] paper, which focused on estimating continuous properties, we estimate the probability of encountering categorical units, or reactive facies. This requires some subtle changes to the *Chen et al.* [2001] method for estimating the prior distribution. The 2-D prior estimates of reactive facies were created using indicator kriging (GSLIB [*Deutsch and Journel*, 1998]) conditioned to reactive facies probabilities estimates extracted from log data. This indicator kriging provides the probability of encountering reactive facies, as a function of position, based on wellbore data only.

[29] The likelihood function, which links the geophysical attributes to the reactive facies, is estimated using the normal linear regression method of *Chen et al.* [2001]. Also different from the *Chen et al.* [2001] approach, the reactive facies were represented as a treatment variable, or bias term, within the regression since they are categorical variables. Assuming that the probability density functions (pdf) of the conditional probabilities are described by a normal distribution, one can utilize a normal linear regression model to estimate the mean and variance required to completely describe the likelihood function. The regression model utilizes collocated facies, GPR and seismic velocity,

and GPR attenuation data. In our categorical system we assign the facies a binary value of 1 or 0, where 1 indicates that the facies exists at that location and 0 if other facies exist at that location. These categorical variables are included in the normal linear regression model as categorical, or treatment, variable [e.g., *Ott and Longnecker*, 2001]. The procedure that we use to obtain the likelihood models from the collocated data is a stepwise deletion model selection process. We start from a quadratic full model and deleting terms that are statistically not significant using a stepwise analysis approach. In the process geophysical attributes that are not contributing sufficiently to the estimation are dropped. For example, to find the optimal regression model, an initial model of GPR velocity (G), as a function of a particular reactive facies (F_i), seismic velocity (S) and GPR attenuation (A), was constructed with polynomial powers up to a power of 2:

$$\begin{aligned} G(F_i, S, A) &= \beta_0 + \beta_1 \bullet F_i + \beta_2 \bullet A + \beta_3 \bullet S + \beta_4 \bullet A \bullet S \\ &+ \beta_5 \bullet F_i \bullet A + \beta_6 \bullet Fi \bullet S + \beta_7 \bullet F_i \bullet S \bullet A + \beta_8 \bullet A^2 \\ &+ \beta_9 \bullet S^2 + \beta_{10} \bullet Fi \bullet A^2 + \beta_{11} \bullet F_i \bullet S^2 + \beta_{12} \bullet S^2 A^2 \\ &+ \beta_{13} \bullet F_i \bullet S \bullet A^2 + \beta_{14} \bullet F_i \bullet S^2 \bullet A + \beta_{15} \bullet F_i \bullet S^2 \bullet A^2 \\ &(F = 1 \text{ or } 0). \end{aligned} \tag{2}$$

After finding the coefficients ($\beta_{i = 0,1,2\ldots15}$) for this polynomial that best fit G, the terms of the polynomial equation with the lowest significance factor is eliminated and then the remaining polynomial terms are refit to the data. This model selection process iterates until all remaining terms fit to a ($p = 0.01$) significance level. This normal regression model can then be used to calculate the mean and variance (e.g., G as a function of A, S and F), and the mean and variance can then be used to calculate the normal pdf. If more than two reactive facies exist, an independent regression model can be used for each facies, because each facies is exclusive of other facies. In the example of two facies, only one model is needed since the absence of one facies automatically indicates the presences of the other facie. To estimate the posterior facies using geophysical data, we define the posterior probability for a categorical facies variable as

$$p(F_i) = \frac{p(F_i|A, G, S)}{\sum_{j=0\ldots N} p(F_j|A, G, S)}, \tag{3}$$

where F_i is facies whose probability is being calculated of the N number of facies (here N = 2).

[30] After estimation of the posterior reactive facies distribution through solving equation (3) numerically, we can obtain the conditional probability of the facies-based reactive transport properties given the probability of the facies at each pixel. This is accomplished by integrating the posterior estimate of the reactive facies with the property distributions for those facies to provide conditional pdf's of fine content, porosity, hydraulic conductivity, and Al:Fe ratios. These distributions allow for the ability to draw multiple possible realizations for parameterizing reactive transport models. For simplicity, we provide only the mean of the distribution at each pixel for figures and simulation.

2.3.3. Reactive Transport Simulations

[31] Reactive transport simulations were carried out with the code TOUGHREACT [*Xu et al.*, 2011] to test the influence of geophysically estimated reactive facies and associated physical and geochemical properties on the predicted migration of an acidic-U plume in the F-Area Savannah River Site. These exploratory simulations were run along the same 2-D tomography transects that were used to estimate reactive facies at the local scale (Figure 3), although lateral extrapolations of the estimates were performed to allow the simulations to be conducted through a rectangular region. As will be described in section 3.3, the geophysically obtained distributions of porosity, permeability, and mineral volumetric fractions (quartz, kaolinite and goethite) were used to parameterize the model. The estimated probability density functions of Al:Fe ratios were used to estimate the proportions of kaolinite and goethite (assuming no Al substitution in goethite). The volume fractions of these minerals were then used to compute corresponding (heterogeneous) fields of surface area and cation exchange capacity (CEC, using specific surface areas for goethite and kaolinite, and CEC data for kaolinite from *Dong et al.* [2012]). Simulations were then performed considering the following cases of property distributions within the modeled domain: (1) fully heterogeneous model (abbreviated here as the "Hetero" case), with heterogeneous fields of permeability, porosity, and mineral volume fractions, (2) fully homogeneous model (abbreviated here as the "Homo" case), with homogeneous property values calculated by taking the mean of the heterogeneous property fields (using geometric mean for permeability and arithmetic mean for porosity and mineral volume fractions), (3) heterogeneous permeability only (abbreviated here as the "Hydrofacies" case), with heterogeneities only affecting flow, and mean values taken for porosity and mineral amounts, and (4) heterogeneous porosity and mineral volume fractions (abbreviated here as the "Chemofacies" case), resulting in heterogeneous solid-to-water ratios that directly affect sorption and exchange reactions, while a geometric mean value is used for homogeneous permeability.

[32] The modeled geochemical reaction network for the F-Area from *Dong et al.* [2012] was used to simulate the U pH-dependent adsorption. The reaction network consists of nine components (U, H^+, nitrate, Al, Ca, Mg, Na, K, and H_2O) and includes the formation of aqueous complexes as well as surface and exchange species for the adsorption of H+ and U onto kaolinite and goethite (the latter using data primarily from *Heidmann et al.* [2005] and *Sherman et al.* [2008]). Initial steady state conditions in the flow regime were applied in the reactive transport simulations, with constant positive and negative flow rates imposed on the left and right boundaries of the modeled domain, respectively, with values determined to reproduce observed pore velocities at the site. A scenario involving two infiltration stages was simulated (based on the historical basin operation in the F-Area SRS): (1) stage I (seepage), where the domain is flushed with by an acidic-U solution for a period of 35 years (seepage solution, Table 1), and (2) stage II (capping), where the domain is flushed by the (background) groundwater after the basin closure (background solution, Table 1).

Table 1. Chemical Composition for Background and Seepage Solutions Assumed in the Reactive Transport Simulations[a]

	Background Solution[b]	Seepage Solution[c]
pH	5.4	2.3
U(VI)	10^{-13}	3.1×10^{-5}
Ca	5.5×10^{-3}	1.25×10^{-5}
Na	2.8×10^{-4}	4.1×10^{-3}
Si	1.8×10^{-4}	1.2×10^{-4}
TIC[d]	3.1×10^{-5}	2.5×10^{-5}
Nitrate	10^{-5}	10^{-2}
Al	2.7×10^{-8}	10^{-4}
Fe(III)	2.47×10^{-16}	4.7×10^{-7}
Ionic strength	1.1×10^{-2}	1.04×10^{-2}
P_{CO2} (atm)	3.4×10^{-4}	3.4×10^{-4}

[a]All concentrations (except pH) are in mol kg w^{-1}.
[b]Estimated from site-specific data and assuming equilibrium with kaolinite and goethite at equilibrium with atmospheric CO_2 concentrations.
[c]Based on *Killian et al.* [1986].
[d]Total inorganic carbon.

3. Analysis and Results

3.1. Identification and Distribution of Reactive Facies

[33] The statistical analysis of F-Area data sets revealed significant correlations between geophysical attributes, properties controlling reactive transport, and depositional facies. We found that the fine content was highly correlated to hydraulic conductivity ($R^2 = 0.53$), to the Al:Fe ratio ($R^2 = 0.75$) and to surface area ($R^2 = 0.73$; Figure 6). As shown in Figure 6, there is a nonlinear relationship between hydraulic conductivity and percent fine content; a positive linear correlation between Al:Fe ratio and percent fines; and a positive linear relationship between surface area (measured by BET) and percent fines. As described in section 2.2.1, we chose to explore the ratio of Al to Fe because those elements provide a proxy of the amount of kaolinite ($Al_2Si_2O_5OH_4$) and goethite (FeOOH) within the bulk sample, which were identified as critical controls for U sorption at the F-Area [*Dong et al.*, 2012]. Because of the expected sensitivity of both GPR and seismic attributes to texture, this strong correlation between the reactive properties and fines suggests that GPR and seismic methods can potentially be useful for estimating reactive properties. However, direct correlation between the GPR and seismic attributes to point (core) measurements of fine content revealed only weak correlations (Figure 7), possibly hindered by the lack of colocated data, sample disturbance, and/or the differing support scale of the geophysical methods.

[34] We also performed statistical analysis of the physical, hydraulic, sediment geochemical, and geophysical parameters as a function of depositional facies. Figure 8 reveals that the two main depositional facies at the site, a barrier beach facies and a lagoonal facies, indeed have distinct distributions of fine content, hydraulic conductivity, and Al:Fe ratios. Marked contrasts in porosity were also observed between the two facies (Figure 9).

[35] This analysis establishes that two reactive facies exist at the F-Area, which have unique distributions of hydraulic and geochemical parameters as summarized in Table 2. At this site, the reactive facies are coincident with depositional facies. We stress that the correspondence is not a necessary condition for reactive facies. For example, in some cases, depositional facies may not be hydraulically or geochemically distinct. In other cases, post depositional alteration through natural processes (as described by *Kleineidam et al.* [1999]) or through anthropogenic processes (such as introduction of a plume) may alter reactive properties that comprise reactive facies. We stress that a reactive facies is a subsurface unit that has a distinct distribution, relative to surrounding units, of reactive transport properties that have been established to be important for the particular site in controlling reactive transport. At the fringe of the plume region in the F-Area, laboratory analysis was used to establish the properties that control reactive transport and statistical analysis of field data has established that the reactive facies are coincident with depositional facies. In subsequent discussions, we will refer to these two reactive facies as the "barrier beach reactive facies" and the "lagoonal reactive facies."

[36] Having established that two reactive facies exist and are coincident with depositional facies, we then explored the relationships between geophysical attributes and depositional facies. The inverted geophysical attributes of seismic *P* wave velocity, radar velocity, and radar attenuation were extracted from the tomograms at positions near the

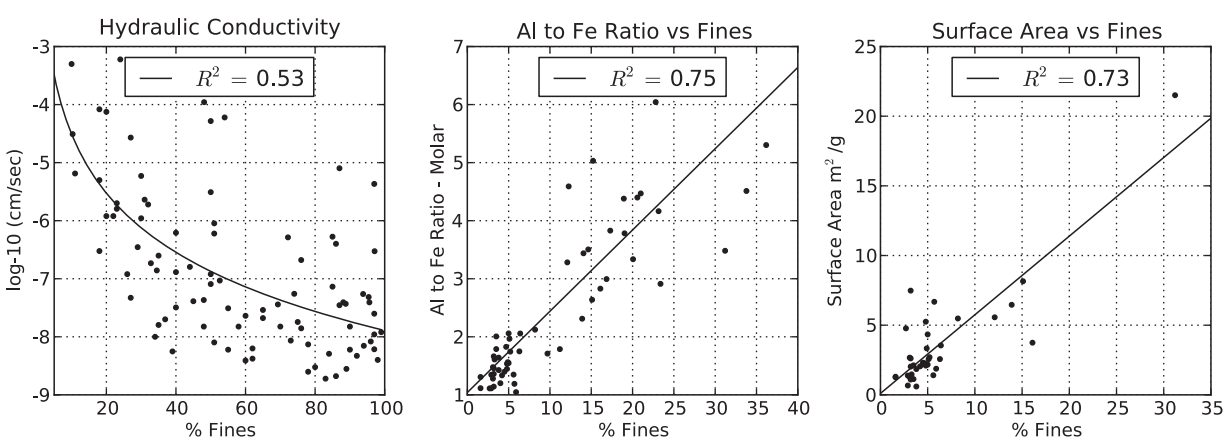

Figure 6. Scatterplots of laboratory measurements versus percent fines. (left) Hydraulic conductivity against percent fines, (middle) Al to Fe ratio versus percent fines, and (right) total surface area versus percent fines.

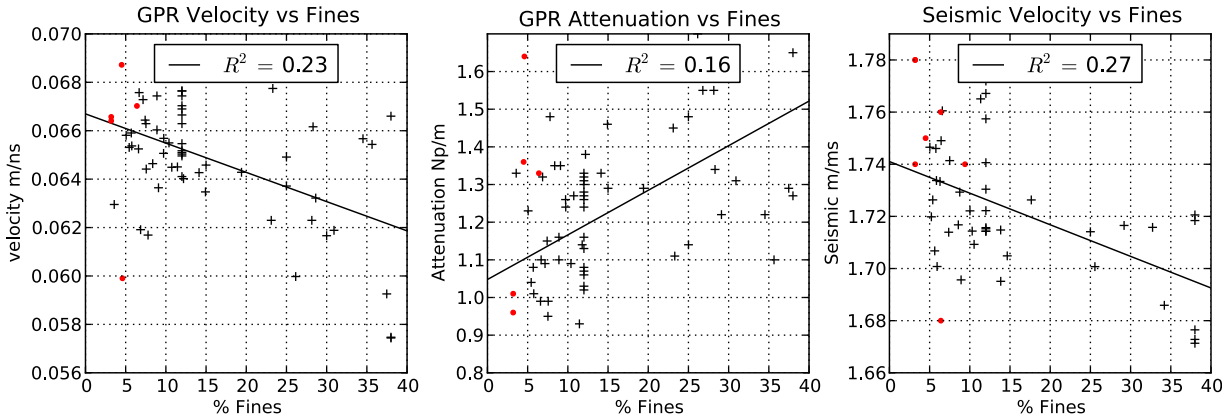

Figure 7. Scatterplots of geophysical attributes versus percent fines, revealing weak relationships when the geophysical attributes are compared to individual core (point) measurements, which are considered as a continuum. Black crosses represent interpolated data from FSB-120AR (∼1.5 m away), and red dots represent collocated measurements. (left) GPR velocity versus percent fines, (middle) GPR attenuation versus percent fines. and (right) seismic *P* wave velocity versus percent fines.

wellbore and were compared with collocated depositional facies at cells along wells FAW-1, 120A, and 120C (refer to Figure 2 for location and Figure 5 for an example). We also compared the geophysical logs (gamma and electrical conductivity) to the facies described at the same wellbores (refer to Figure 4). Figure 10 and Table 2 show that the depositional facies are geophysically distinguishable. The lagoonal facies had a relatively lower seismic velocity, lower radar velocity, higher gamma count, higher electrical conductivity and higher radar attenuation relative to the beach barrier depositional facies, as is summarized in Table 2. Note that by comparing the geophysical attributes to facies rather than the individual (point-based) properties (refer to Figure 7) the differences in support scale and sample disturbance concerns were minimized and the correspondence improved.

3.2. Distributions of Reactive Facies and Associated Properties at the Local Field Scale

[37] Our data mining analysis has provided insights into the existence of two distinctive reactive facies related to depositional processes, and that these facies can be distinguished on the basis of geophysical responses. The existence of only two reactive facies simplifies our estimation problems to a bimodal system. This simplification allows us to invoke the binomial distribution function in the estimation procedure and to utilize the already interpreted depositional facies logs together with the tomographic geophysical data to estimate reactive facies distributions at the field scale. Here we take a two-step approach of (1) estimating the distribution of the reactive-facies using geophysics in a Bayesian estimation framework and then (2) estimating hydrological and reactive transport properties associated with the reactive facies along 2-D tomographic transects. To assess the approach, we compare our geophysically obtained estimates with independent results obtained through laboratory XRF analysis, textural analysis and titration experiments. We also use the geophysically obtained estimates to parameterize a local-scale reactive transport model, and carry out simulations to illustrate the control of the identified reactive facies on plume transport.

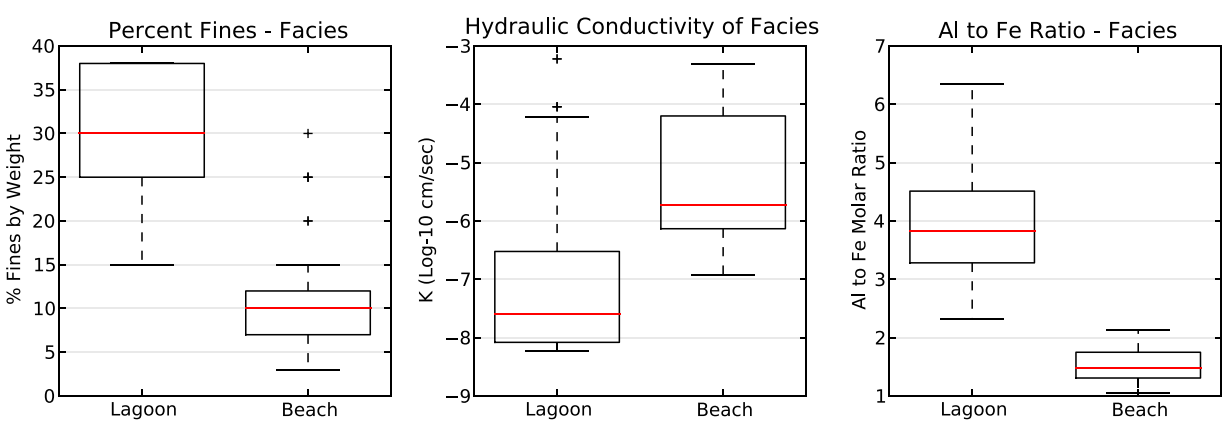

Figure 8. Reactive transport property distribution as a function of depositional facies. (left) Distributions of percent fine content as a function of depositional facies, (middle) distribution of hydraulic conductivity as a function of depositional facies, and (right) distribution of ratio of Al to Fe as a function of depositional facies.

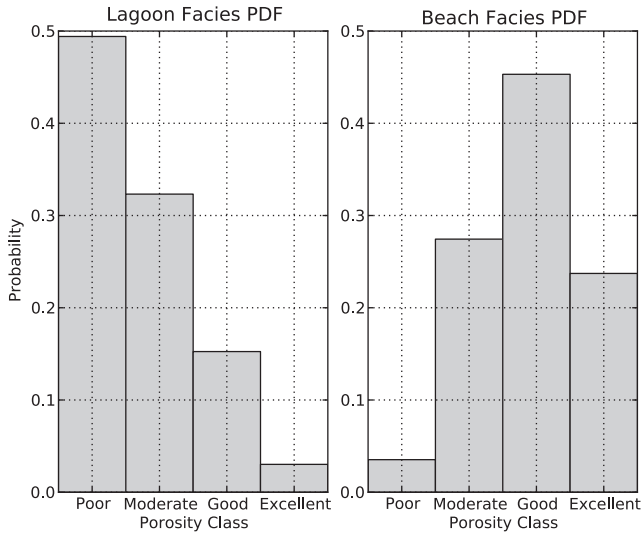

Figure 9. Probability density functions of porosity classes (poor, <5%; moderate 5%–15%; good, 15%–30%; excellent, >30%) for the lagoon and beach depositional facies, as determined from binocular microscope analysis [*Smits et al.*, 1997].

[38] Figure 11 shows the probability of encountering the lagoonal facies obtained through solving the Bayesian formulation given in equation (3) using the prior distribution of facies, the established likelihood functions, and the geophysical attribute estimates (seismic velocity and radar velocity and attenuation) along the same two tomographic transects shown in Figure 3. Figures 3 and 11 show that the majority of the study section is interpreted to be the barrier beach reactive facies (blue), with some lagoonal reactive facies distributed between 23 to 38 m depth.

[39] Figure 12 shows the mean estimates of the individual flow and transport properties associated with the estimated reactive facies along the same two local-scale tomographic transects. Figure 12 shows that in areas where the probability of either reactive facies is very high, the estimate approaches the mean of the distributions for each property. In areas of high variance in the reactive facies estimate, the property estimates are weighted averages of the properties of both facies.

[40] To test the predictive power of the Bayesian method for estimating specific properties associated with the reactive facies, we compared the geophyiscally obtained estimates with measurements obtained using two independent data sets. Figure 13 shows a comparison of the Bayesian estimates of percent fines with that retrieved from the historical data, and the Bayesian estimates of the Al:Fe ratio relative to those obtained using the XRF method, described in section 2.2.1, from the retrieved core samples. Unfortunately, all of the texture and XRF measurements were performed on samples retrieved from the beach facies, and as such the measurements are fairly homogeneous. The deepest of the samples is located in a transitional area with increased probability of the lagoonal reactive facies, and show higher levels of fines (11%). Even so, all of measurements fall within the 95% confidence interval of our estimates. We note that there is a systematic overestimation of the percent fines, potentially due to the differences in grain size analysis of our current core analysis (used for verification here) and the historical data (used to generate the conditional probabilities), as was described in section 2.2.2. Despite the disparate measurement support scales of a "point" core measurement and the geophysical estimates, as was previously discussed, these comparisons suggest that the reactive parameters estimated using the Bayesian approach within the beach barrier are reasonable.

[41] We also compared the geophysically obtained estimates of reactive facies with independent reactive facies information obtained using the base titration approach described in section 2.2.1. Again, because pH plays an important role in the adsorption of uranium, differences in sediment titration data are thought to be indicative of reactive behavior. These titrations were performed on a limited number of cores retrieved from our drilling campaign, including cores F (located in the interpreted barrier beach reactive facies) and G (located near the interpreted lagoonal reactive facies) as indicated on Figure 11. Figure 14 shows that the sample located near the lagoonal reactive facies reveals a higher base consumption rate relative to the sample located in the barrier beach reactive facies. Although these data are sparse, they allow an independent assessment of the value of the reactive facies concept and estimation approach.

3.3. Reactive Transport Simulations Using the Reactive Facies Estimates

[42] Here, we illustrate how the reactive facies estimates can be used to parameterize a reactive transport model, and explore through simulations the influence of reactive-facies-based heterogeneity on U plume transport. To facilitate simulation through a 2-D domain, the bottom left of

Table 2. Mean, SD, and Bootstrap Significance Level of Physical, Hydraulic, Mineralogical, and Geophysical Property Distributions of the Two Identified Reactive Facies

Property	Lagoonal Reactive Facies	Barrier Beach Reactive Facies	Significance Level[a]
Fine content	30.5, ±6.75	10.8, ±5.09	p = 0.0
Hydraulic conductivity (cm s^{-1})	6.54×10^{-6}, $\pm 1.90 \times 10^{-5}$	9.19×10^{-5}, $\pm 1.75 \times 10^{-4}$	p = 0.00558
Porosity[b]	moderate to poor	good to moderate	N/A
Al:Fe molar ratio	3.981, ±1.038	1.528, ±0.299	p = 0.0
Seismic velocity (m ms^{-1})	1.697, ±0.0183	1.730, ±0.0213	p = 0.00018
Radar velocity (m ns^{-1})	0.0636, ±0.00294	0.0654, ±0.00192	p = 0.0
Radar attenuation (Np m^{-1})	1.424, ±0.209	1.187, ±0.1476	p = 0.00802

[a]The bootstrap significance level is the probability that the alternative hypothesis is true (i.e., both distributions of the property for facies are the same [*Efron and Tibshirani*, 1993]).
[b]The porosity classes are defined as less than 5% for poor, 5%–15% for moderate, and 15%–30% for good.

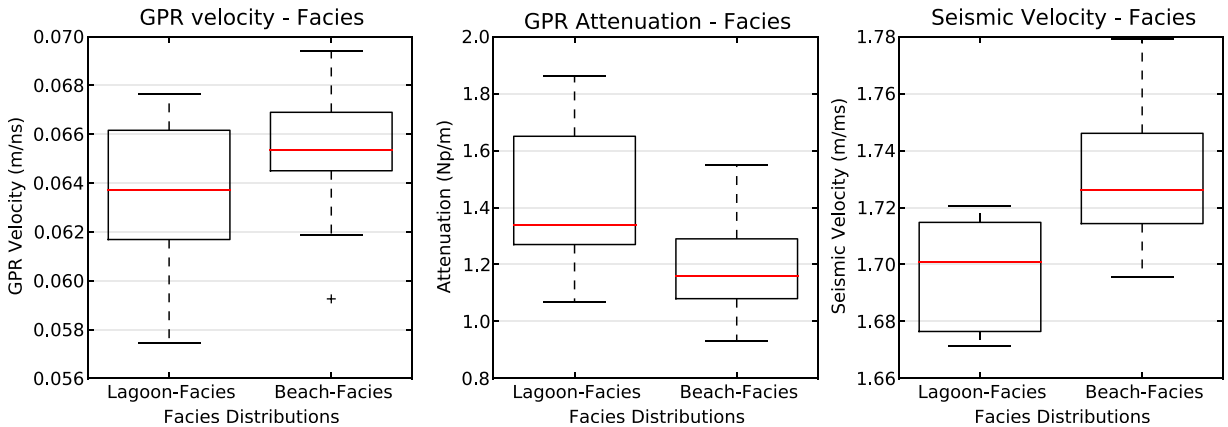

Figure 10. Geophysical attribute distributions as a function of depositional facies. (left) Distributions of GPR velocity as a function of facies, (middle) distribution of GPR attenuation as a function of facies, and (right) distribution of seismic velocity as a function of facies.

the region shown in Figure 12 was extrapolated using kriging to create a heterogeneous rectangular (exploratory) model domain. The geophysically estimated transport properties (or transformation of those properties obtained as described in section 2.3.3) were used to parameterize the reactive transport model (Figure 15). Results of simulations using these fields of properties are shown on Figure 16, including a comparison of modeled results for previously described cases of heterogeneities: fully heterogeneous Hetero case, fully homogenous Homo case, heterogeneous reactive properties (solid-to-water ratios) Chemofacies case, and heterogeneous permeability Hydrofacies case.

[43] Computed spatial distributions of pH and concentrations of U at different times are shown in Figures 16a and 16b, respectively, for the Hetero case. The steady state pore velocity distribution for this case (Figure 16c) is consistent with that observed for the UUTRA aquifer system in the F-Area ($\sim$130 m yr^{-1}). The computed temporal evolution of the normalized mass of U over the entire simulated time period is shown in Figure 16d. To show the impact of heterogeneities on flow and reactive processes, results for the Hetero, Homo, Chemofacies and Hydrofacies cases are compared in this plot. Breakthrough curves for nitrate, pH and U at different locations (i.e., at points B1 and B2 in Figure 16a) are shown in Figures 16e–16g, respectively. In these plots, the breakthrough curves corresponding to the two reactive facies (Hetero) case are compared with the fully homogeneous (Homo) case.

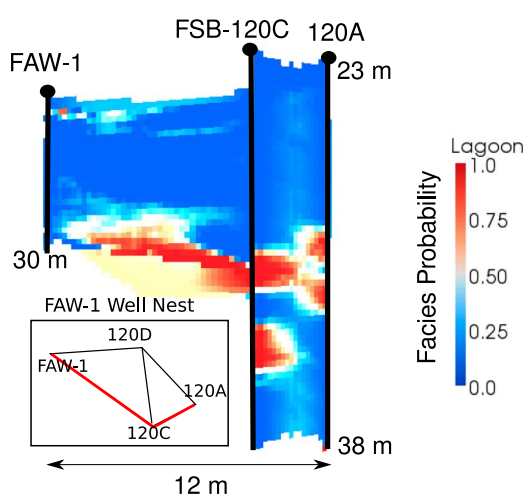

Figure 11. The posterior probability of a lagoonal facies in the FAW-1 well nest. Red areas indicate a high probability of the presence of the lagoonal facies, and blue areas indicate a high probability of the beach-barrier reactive facies.

[44] Analyses of these model results reveal the effect of the reactive facies on both localized plume evolution and total U mass attenuation in the subsurface. Solute transport in the beach reactive facies is advection dominated, whereas it is a lesser transport process in the lagoonal reactive facies as a result of the low permeabilities (see Figures 16a and 16b). In addition, contaminant (U and H^+) loading and retardation in the lagoonal reactive facies are enhanced by the higher surface area (solid-to-water ratio) in this facies, which yields a larger number of sites for sorption and exchange (see goethite and kaolinite volumetric distributions in Figures 15e and 15f) relative to the barrier beach reactive facies. It should be noted that the predicted pH and U concentrations after 35 years, at the end of stage I (seepage), show nearly homogenous U and pH distributions (Figures 16a and 16b). This is because during seepage, sorption sites become saturated by the massive influx of U and H^+, at which point sorption no longer controls the aqueous concentrations of these contaminants. However, following stage II (capping), pH partly rebounds when the background groundwater flushes the domain. During this stage, the pH rebound is much slower in the lagoonal reactive facies (Figure 16f), and a significant mass of U persists in the modeled domain (e.g., compare Hetero and Homo cases in Figure 16d).

[45] The slower rates of pH rebound in the lagoonal reactive facies are consistent with base titration results observed for a sediment sample that was collected in a transitional area with increased probability of the lagoonal reactive facies (Figure 14). As would be expected, the computed normalized mass of U in the heterogeneous reactive facies model domain (Hetero) persists over a much longer time period than in the averaged homogeneous model domain (Homo; Figure 16d), because of increased loading and slow

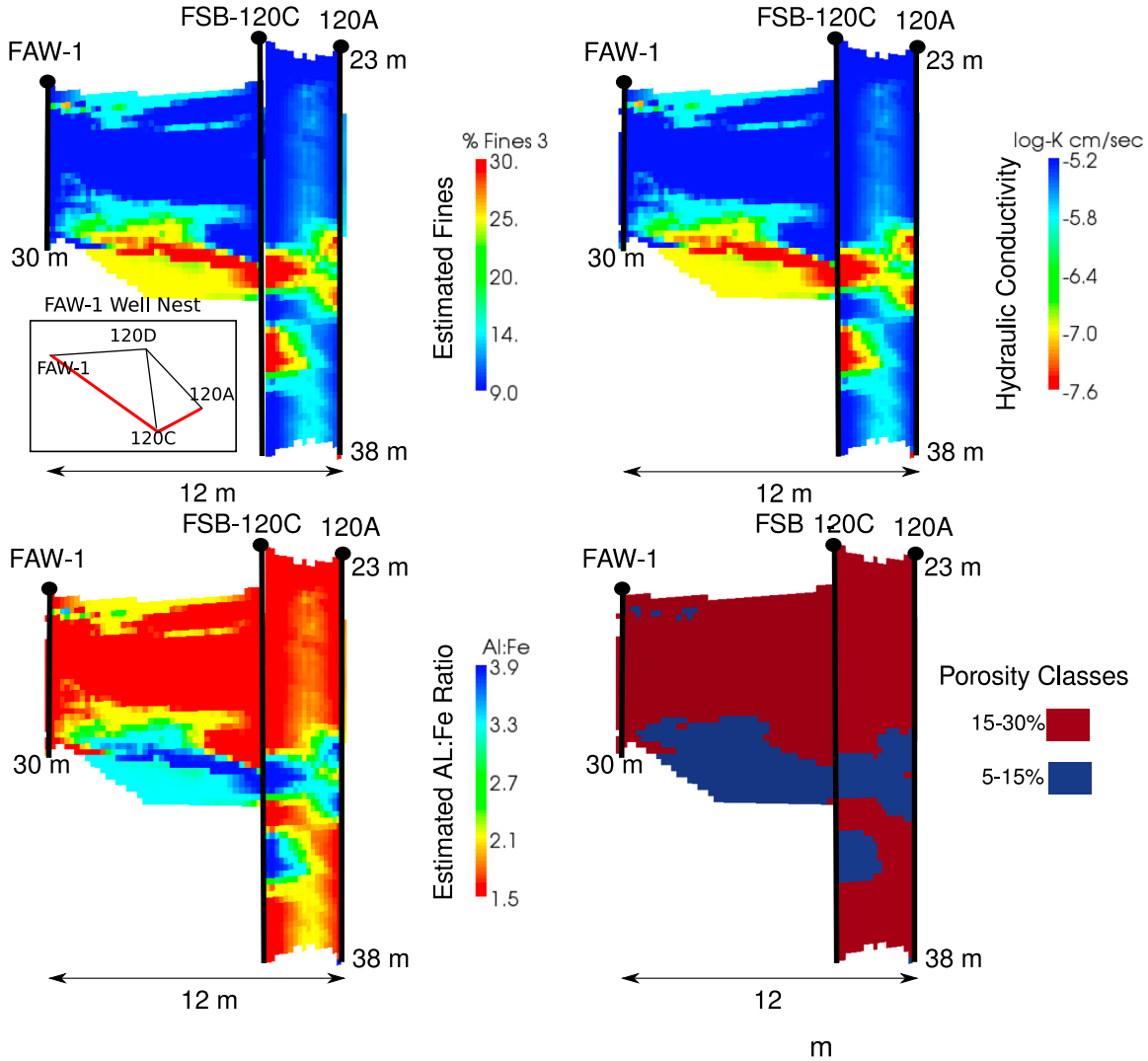

Figure 12. The mean estimates of (top left) reactive facies based fine content, (top right) hydraulic conductivity, (bottom left) Al:Fe ratio, and (bottom right) porosity along 2-D transects between the FAW-1 FSB-120C and FSB-120C and FSB-120A wells.

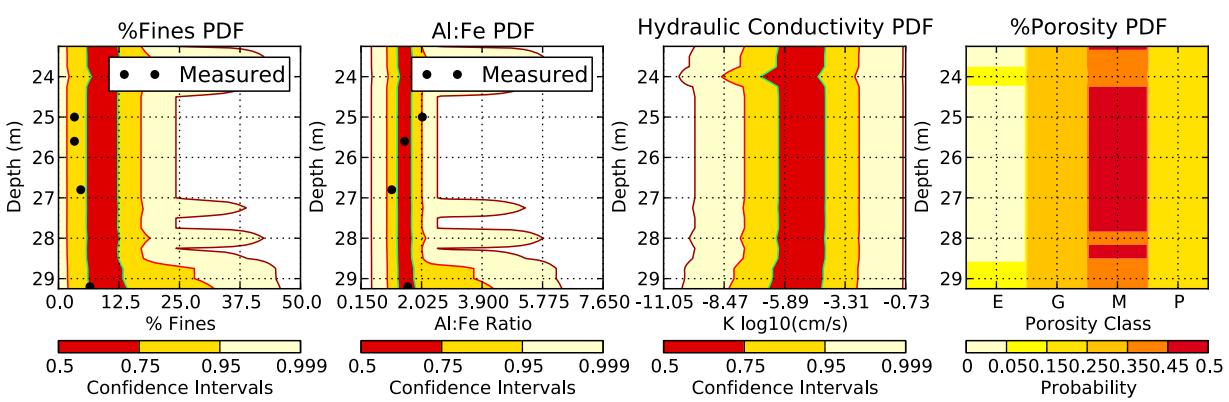

Figure 13. Comparison of measured and estimated physiochemical property values. The contour maps show the confidence intervals of the physiochemical properties as a function of depth immediately adjacent to the well FAW-1. The black circles represent direct measurements.

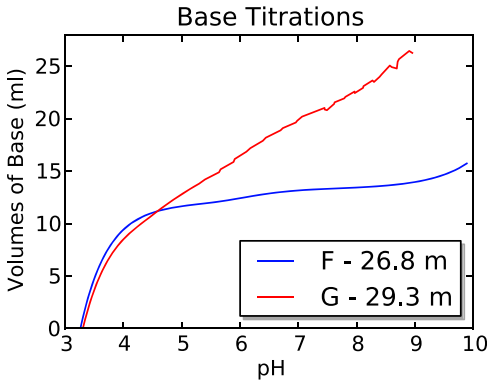

Figure 14. Base titration from samples FAW-1F (in the barrier beach reactive facies) and FAW-1G (near the lagoonal reactive facies; see Figure 11). Differences in base volumes as a function of pH indicate differing surface charge characteristics associated with the reactive facies.

desorption in areas of high solid-to-water ratios and low permeability. Interestingly, there are marked contrasts in Figure 16d between the Hetero and Hydrofacies cases but little difference between the Homo and Chemofacies cases, indicating that the combination of permeability and reactive (mineral volume fractions plus porosity) heterogeneities in this case has more an effect than reactive heterogeneities alone. This is because zones of low permeability tend to be more reaction dominated than transport dominated (i.e., display increased fluid residence times [e.g., *Glassley et al.*, 2002; *Seeboonruang and Ginn*, 2006a, 2006b]), and therefore zones of low permeability (in the heterogeneous permeability case) with elevated solid-to-water ratios display more reactivity than in the case of higher homogenous permeability with similarly elevated solid-to-water ratios. These model results indicate that not only permeability heterogeneity is important in predicting plume transport, but that heterogeneous solid-to-water ratios (introduced by input heterogeneous fields of mineral volume fractions and porosity, and resulting in heterogeneous surface areas for sorption and exchange) also exert a key control when coupled with heterogeneous permeability. This example highlights the utility of reactive facies as an approach for parameterizing reactive transport models with coupled physical and chemical heterogeneities toward improved field-scale predictions of plume transport.

3.4. Future Directions

[46] This study has demonstrated our ability to identify and extrapolate reactive facies between Savannah River Site F-Area wells at the local scale (tens of meters) using cross-hole geophysical data sets and Bayesian methods. However, to be useful for parameterizing reactive transport models over plume scales, two additional problems must be tackled. First, it is necessary to understand the stationarity of the relationship between the reactive facies, the reactive transport properties, and the geophysical signatures. Here, we have explored these relationships for a region of the study site located on the contaminant plume fringe (refer to Figure 2). An understanding of the relationships between reactive facies properties and geophysical attributes in the center of the plume, where the minerals have been bathed in acid for several decades, is required for application of this method over the entire plume region; this research is ongoing through analysis of data collected at the local scale site near wellbore FAW-5. The second problem is extrapolation of the reactive facies estimates to larger spatial regions, as is needed to parameterize site-wide reactive transport models. Such extrapolation requires geophysical methods that have sensitivity to the reactive facies but have greater spatial coverage than the cross-well tomographic data used herein. Surface geophysical methods, such as electrical resistivity tomography and seismic reflection data, can potentially fill this gap. Seismic data already acquired at the site show a significant response to the major changes in depositional processes that define the stratigraphic units at the site. Ongoing efforts are underway to address the stationarity issue and to build upon the methodology presented here to develop a multiscale reactive facies Bayesian estimation methodology that can extend the concepts developed here to larger spatial scales.

4. Discussion and Conclusions

[47] The concept of reactive facies is based on the hypothesis that intermediate to large scale subsurface units can be identified that have linked distributions of properties that influence reactive transport, including both physical and chemical properties. This concept can potentially simplify the task of characterizing the reactive transport properties of a complex geological system over field-relevant scales by exploiting the nonrandom distribution of subsurface units and by utilizing geophysical methods, which often can be used to distinguish between geological units.

[48] Here we developed and tested a Bayesian methodology for using geophysical data and laboratory derived insights to provide and distribute estimates of the reactive facies; their associated hydraulic, physical, and mineralogical properties; and their associated uncertainties. Even in the absence of extensive calibration data and applied over a relatively homogeneous subsurface interval, our study suggests that reactive facies can be geophysically identifiable. Comparison of the geophysically obtained reactive facies estimates with sparse independent measurements suggests that the estimation approach is reasonable. Additionally, reactive transport simulations highlight the potential value of the reactive facies approach for parameterizing models used to predict plume mobility.

[49] The reactive facies approach we developed and tested at the F-Area is generalizable to other sites, conditions, and data sets. While we exploited the relationships between depositional facies and geophysical attributes to distribute reactive transport properties, other types of subsurface units or alterations may exert more influence on reactive transport at other sites. In some cases, it may be more useful to explore the relationships between lithological properties and reactive properties, for example a reduced sandstone versus an oxidized sandstone, or an acidized sandstone versus a natural sandstone. As we discussed in section 2.2.1, critical to the success of the approach is the a priori development of an understanding of the key controls of contaminant reactivity at the site under consideration, and thus the properties of the reactive facies are site specific.

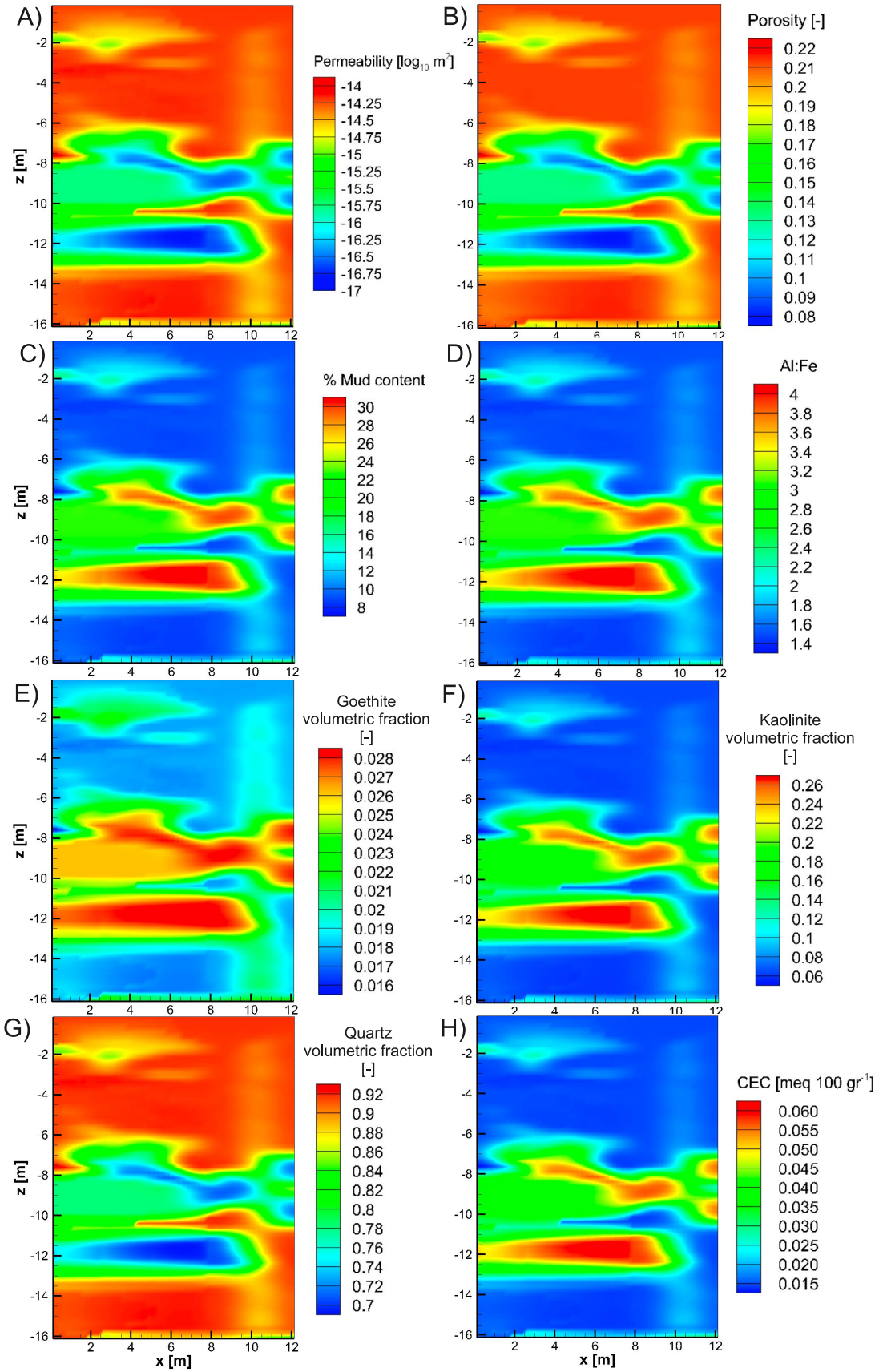

Figure 15. Geophyiscally obtained hydrological and geochemical parameter distributions: (a) permeability, (b) porosity, (c) mud percentage content, (d) Al:Fe, (e–g) goethite, kaolinite, and quartz volumetric content, respectively, and (h) cation exchange capacity.

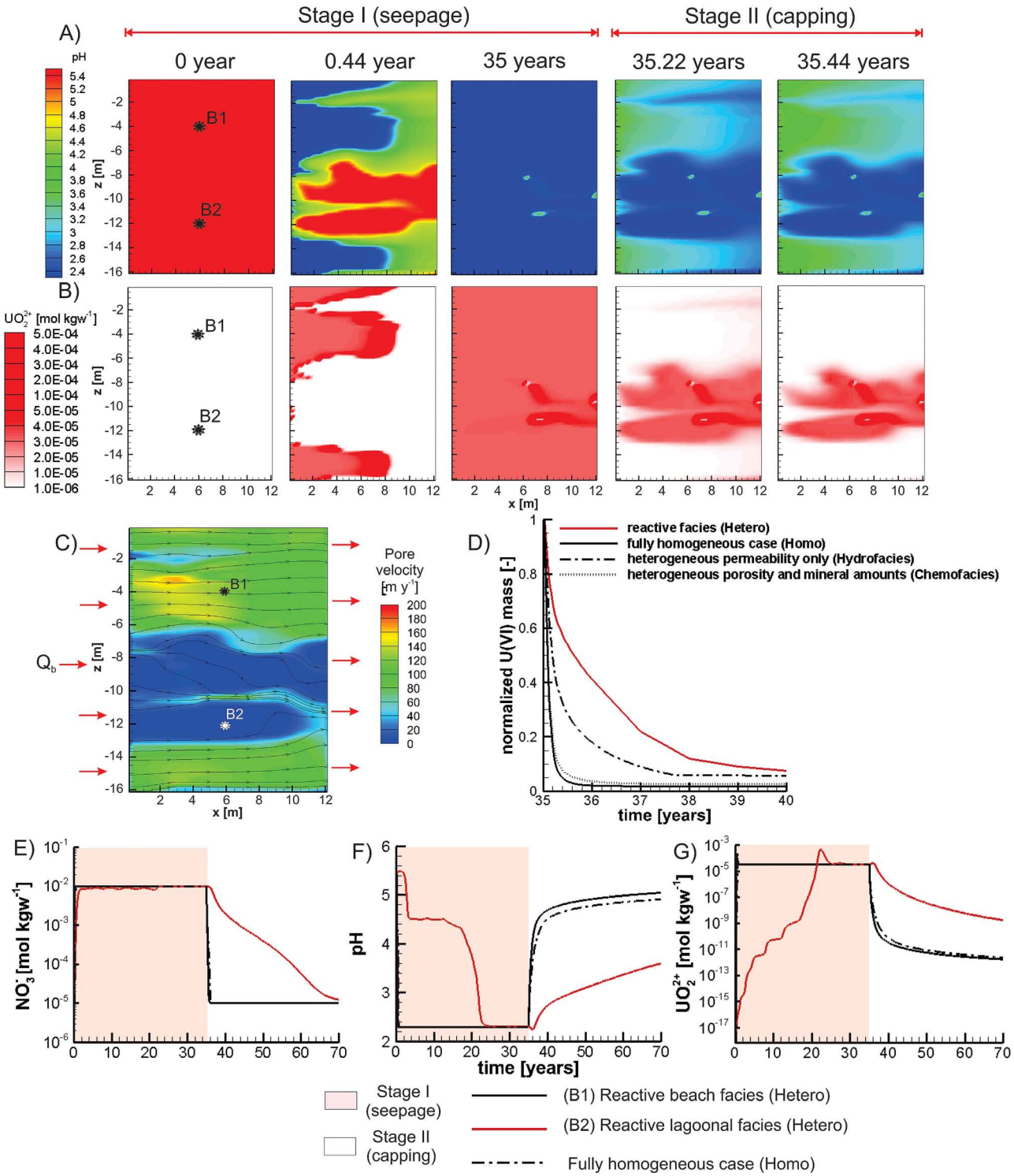

Figure 16. Reactive transport simulation results. (a and b) Spatial distribution of pH and total concentration of U(VI) at 0, 0.44, 35, 35.22, and 35.44 years, respectively. (c) Pore velocity distribution. (d) Temporal evolution of the normalized mass of U for stage II (capping). Breakthrough curves at B1 and B2 locations for (e) nitrates, (f) pH, and (g) U.

[50] A facies based approach to parameterizing reactive transport models has inherent advantages over characterizing and distributing independent, point-based measurements. Because a facies approach essentially compresses the large number of properties used in reactive transport prediction into a small number of facies, application to larger regions having more heterogeneity is expected to increase the utility of the reactive facies method for field-scale characterization. Although the point-to-point comparison of geophysical attributes with the physical, geochemical,

and hydraulic properties showed somewhat limited correlation, our study showed that geophysical attributes could distinguish between depositional facies, which was then exploited to estimate and spatially extrapolate the reactive facies and their associated property distributions. The use of facies-based approach for estimating reactive transport properties circumvented the often-encountered problem of developing petrophysical relationships between geophysical and well-based measurements, which often have different support scales and different levels of disturbance. Small-scale heterogeneity, below the support scale of geophysical methods, also play an important role in large-scale reactive transport and perhaps may be treated with equivalent effective media developed from core samples that too can be correlated to facies. Although additional effort is needed to fully validate and extend the method to larger spatial scales, our study suggests that the reactive facies is a useful concept, that the estimation approach is reasonable, and that the larger scale geophysical field data offers a vehicle for extension to plume-relevant regions. Because quantification of reactive transport properties or behaviors are traditionally difficult to obtain, this methodology holds great potential for improving predictions of contaminant transport in heterogeneous subsurface environments, such as at the Savannah River F-Area

[51] Certainly, research opportunities exist to further test the developed estimation procedure for tractably characterizing reactive transport properties over field-relevant scales at locations having a wider range of heterogeneity and different conditions relative to the F-Area.

[52] **Acknowledgments.** Our study was supported as part of the Subsurface Science Scientific Focus Area funded by the U.S. Department of Energy, Office of Science, Office of Biological and Environmental Research under Award Number DE-AC02-05CH11231 to the LBNL Sustainable Systems SFA. We also acknowledge support from EM-32 for field support at the F-Area Applied Field Study Site, including acquisition of surface seismic data. We sincerely appreciate the efforts of John E. Peterson (LBNL), Kenneth H. Williams (LBNL) for collecting field geophysical data; Rick Miller (KGS) for collecting and processing the surface seismic data; and Maggie Millings (SRNL) and others for assisting with the field campaigns. Gratitude is also extended to Jiamin Wan (LBNL) and Wenming Dong (LBNL) for geochemical laboratory analysis of F-Area data used to motivate this study.

References

Allen-King, R. M., R. M. Halket, D. R. Gaylord, and M. J. L. Robin (1998), Characterizing the heterogeneity and correlation of perchloroethene sorption and hydraulic conductivity using a facies-based approach, *Water Resour. Res.*, *34*(3), 385–396.

Anderton, R. (1985), Clastic facies models and facies analysis, in *Sedimentology, Recent Developments and Applied Aspects*, edited by P. J. Brenchley and B. P. J. William, pp. 31–47, Blackwell Sci., Oxford, U. K.

Beckie, R., and C. F. Harvey (2002), What does a slug test measure: An investigation of instrument response and the effects of heterogeneity, *Water Resour. Res.*, *38*(12), 1290, doi:10.1029/2001WR001072.

Butler, J. J., Jr. (2005), Hydrogeological methods for estimation of hydraulic conductivity, in *Hydrogeophysics*, edited by Y. Rubin and S. Hubbard, pp. 23–58, Springer, Dordrecht, Netherlands.

Chapelle, F. H. (2001), *Ground-Water Microbiology and Geochemistry*, John Wiley, New York.

Chen, J., S. Hubbard, and Y. Rubin (2001), Estimating hydraulic conductivity at the South Oyster Site from geophysical tomographic data using Bayesian techniques based on the normal linear regression model, *Water Resour. Res.*, *37*(6), 1603–1613.

Chen, J., S. Hubbard, Y. Rubin, C. Murray, E. Roden, and E. Majer (2004), Geochemical characterization using geophysical data: A case study at the South Oyster Bacterial Transport Site in Virginia, *Water Resour. Res.*, *40*, W12412, doi:10.1029/2003WR002883.

Chen, J., S. S. Hubbard, V. Korneev, D. Gaines, G. Baker, and D. Watson (2010), Stochastic inversion of seismic refraction data for estimating watershed-scale aquifer geometry: Development and application to a contaminated aquifer, *Water Resour. Res.*, *46*, W11539, doi:10.1029/2009WR008715.

Day-Lewis, F. D., K. Singha, and A. M. Binley (2005), Applying petrophysical models to radar travel time and electrical resistivity tomograms: Resolution-dependent limitations, *J. Geophys. Res.*, *110*, B08206, doi:10.1029/2004JB003569.

de Marsily, G., F. Delay, J. Gonçalv, P. Renard, V. Teles, and S. Violette (2005), Dealing with spatial heterogeneity, *Hydrogeol. J.*, *13*, 161–183.

Denham, M., and K. M. Vangelas (2009), Biogeochemical gradients as a framework for understanding waste-site evolution, *Remediation*, *19*, 5–17.

Denham, M. E. (1999), SRS geology/hydrogeology environmental information document, *Rep. WSRC-TR-95-0046*, Savannah River Lab., Aiken, S. C.

Deutsch, C. V., and A. G. Journel (1998), *GSLIB: Geostatistical Software Library and User's Guide*, 2nd ed., Oxford Univ. Press, Oxford, U. K.

Dong, W., T. Tokunaga, J. Davis, and J. Wan (2012), Uranium(VI) adsorption and surface complexation modeling under acidic conditions: Background sediments from the F-Area Savannah River Site, *Environ. Sci. Technol.*, *46*(2), 1565–1571, doi:10.1021/es2036256.

Efron, B., and R. J. Tibshirani (1993) *An Introduction to the Bootstrap*, Chapman and Hall, London.

Eggleston, J., and S. Rojstaczar (1998), Identification of large-scale hydraulic conductivity trends and the influence of trends on contaminant transport, *Water Resour. Res.*, *34*(9), 2155–2168.

Falivene, O., P. Arbues, A. Gardiner, J. A. Munoz, and L. Cabrera (2006), Best practice stochastic facies modeling from a channel-fill turbidite sandstone analog (the Quarry outcrop, Eocene Ainsa basin, northeast Spain), *AAPG Bull.*, *90*, 1003–1029.

Ferré, T. P. A., A. Binley, J. Geller, E. Hill, and T. Illangasekare (2005), Hydrogeophysical methods at the laboratory scale, in *Hydrogeophysics*, edited by Y. Rubin and S. S. Hubbard, pp. 441–463, Springer, Dordrecht, Netherlands.

Fogg, G. E., C. D. Noyes, and S. F. Carle (1998), Geologically based model of heterogeneous hydraulic conductivity in an alluvial setting, *Hydrogeol. J.*, *6*, 131–143.

Freeze, A. R., and J. A. Cherry (1979), *Groundwater*, Prentice Hall, Englewood Cliffs, N. J.

Ge, Y., and W. Hendershot (2004), Evaluation of soil surface charge using the back-titration technique, *Soil Sci. Soc. Am. J.*, *68*, 82–88.

Gerilynn, R., Z. Moline, and J. M. Bahr (1995), Estimating spatial distributions of heterogeneous subsurface characteristics by regionalized classification of electrofacies, *Math. Geol.*, *27*(1), 3–22.

Glassley, W. E., A. M. Simmons, and J. R. Kercher (2002), Mineralogical heterogeneity in fractured, porous media and its representation in reactive transport models, *Appl. Geochem.*, *17*, 699–708.

Gohn, G. S. (1988), Late Mesozoic and early Cenozoic geology of the Atlantic coastal plains; North Carolina to Florida, in *The Geology of North America, vol. I-2, The Atlantic Coastal Margin: US*, edited by R. E. Sheridan and J. A. Grow, pp. 107–130, Geol. Soc. of Am., Boulder, Colo.

Hamm, L. L., M. K. Harris, P. A. Thayer, J. S. Haselow, and A. D. Smits (1996), Groundwater flow and tritium migration from the SRS Old Burial Ground to Four Mile Branch, *Rep. WSRC-TR-0037*, Savannah River Lab., Aiken, S. C.

Heidmann, I., I. Christl, C. Leu, and R. Kretzschmar (2005), Competitive sorption of protons and metal cations onto kaolinite: Experiments and modeling, *J. Colloid Interface Sci.*, *282*(2), 270–282.

Heinz, J., S. Kleineidam, G. Teutsch, and T. Aigner (2003), Heterogeneity patterns of Quaternary glaciofluvial gravel bodies (SW-Germany): Application to hydrogeology, *Sediment. Geol.*, *158*(1–2), 1–23.

Hubbard, S., and N. Linde (2010), Hydrogeophysics, in *Treatise on Water Science*, vol. 2, edited by S. Uhlenbrook, chap. 20, pp. 401–434, Elsevier, Amsterdam.

Hubbard, S. S., J. Chen, J. Peterson, E. L. Majer, K. H. Williams, D. J. Swift, B. Mailloux, and Y. Rubin (2001), Hydrogeological characterization of the South Oyster Bacterial Transport Site using geophysical data, *Water Resour. Res.*, *37*(10), 2431–2456.

Hubbard, S. S., K. Williams, M. Conrad, B. Faybishenko, J. Peterson, J. Chen, P. Long, and T. Hazen (2008), Geophysical monitoring of hydrological and biogeochemical transformations associated with Cr(VI) biostimulation, *Environ. Sci. Technol.*, *42*(10), 3757–3765, doi:10.1021/es071702s.

Hyndman, D. W., and S. M. Gorelick (1996), Estimating lithologic and transport properties in three dimensions using seismic and tracer data: The Kesterson aquifer, *Water Resour. Res.*, *32*(9), 2659–2670.

Jean, G. A., J. M. Yarus, G. P. Flach, M. R. Millings, M. K. Harris, R. L. Chambers, and F. H. Syms (2004), Three-dimensional geologic model of southeastern Tertiary coastal-plain sediments, Savannah River Site, South Carolina: An applied geostatistical approach for environmental applications, *Environ. Geosci.*, *11*(4), 205–220.

Killian, T. H., N. L. Kolb, P. Corbo, and I. W. Marine (1986), Environmental information document, F-Area Seepage basins, *Rep. DPST 85-704*, Savannah River Lab., Aiken, S. C.

Kleineidam, S., H. Rügner, and P. Grathwohl (1999), Influence of petrographic composition/organic matter distribution of fluvial aquifer sediments on the sorption of hydrophobic contaminants, *Sediment. Geol.*, *129*(3–4), 311–325.

Klingbeil, R., S. Kleineidam, U. Asprion, T. Aigner, and G. Teutsch (1999), Relating lithofacies to hydrofacies: Outcrop-based hydrogeological characterization of Quaternary gravel deposits, *Sediment. Geol.*, *129*, 299–310.

Kohonen, T., J. Hynninen, J. Kangas, and J. Laaksonen (1996), SOM_PAK: The Self-Organizing Map Program Package, *Tech. Rep. A31*, Lab. of Comput. and Inf. Sci., Helsinki Univ. of Technol., Espoo, Finland.

Koltermann, C. F., and S. M. Gorelick (1996), Heterogeneity in sedimentary deposits: A review of structure-imitating, process-imitating, and descriptive approaches, *Water Resour. Res.*, *32*(9), 2617–2658.

Li, L., C. I. Steefel, M. B. Kowalsky, A. Englert, and S. Hubbard (2010), Effects of physical and geochemical heterogeneities on mineral transformation and biomass accumulation during biostimulation experiments at Rifle, Colorado, *J. Contam. Hydrol.*, *112*, 45–63.

Linde, H., S. Finsterle, and S. Hubbard (2006), Inversion of hydrological tracer test data using tomographic constraints, *Water Resour. Res.*, *42*, W04410, doi:10.1029/2004WR003806.

Looney, B. B., J. W. Fenimore, and J. H. Horton (1972), Operating history and environmental effects of seepage basins in chemical separations areas of the Savannah River plant, *Rep. DPST-72-548*, Savannah River Site, Westinghouse Savannah River Co., Aiken, S. C.

Michael, H. A., H. Li, A. Boucher, J. Caers, and S. M. Gorelick (2010), Combining geologic-process models and geostatistics for conditional simulation of 3-D subsurface heterogeneity, *Water Resour. Res.*, *46*, W05527, doi:10.1029/2009WR008414.

Molz, F. J., G. K. Bowman, S. C. Young, and W. R. Waldrop (1994), Borehole flowmeters-field application and data analysis, *J. Hydrol.*, *163*, 347–371.

Moysey, S., K. Singha, and R. Knight (2005), A framework for inferring field-scale rock physics relationships through numerical simulation, *Geophys. Res. Lett.*, *32*, L08304, doi:10.1029/2004GL022152.

Neal, A. (2004), Ground-penetrating radar and its use in sedimentology: Principles, problems and progress, *Earth Sci. Rev.*, *66*, 261–330.

Ott, R. L., and M. T. Longnecker (2001), *An Introduction to Statistical Methods and Data Analysis*, 5th ed., Duxbury, Pacific Grove, Calif.

Paasche, H., J. Tronicke, K. Holliger, A. G. Green, and H. Maurer (2006), Integration of diverse physical-property models: Subsurface zonation and petrophysical parameter estimation based on fuzzy c-means cluster analyses, *Geophysics*, *71*(3), H33–H44.

Peterson, J. E., Jr. (2001), Pre-inversion corrections and analysis of radar tomographic data, *J. Environ. Eng. Geophys.*, *6*(1), 1–18.

Peterson, J. E., B. N. P. Paulson, and T. V. McEvilly (1985), Applications of algebraic reconstruction to crosshole seismic data, *Geophysics*, *50*, 556–1580.

Poeter, E., and D. R. Gaylord (1990), Influence of aquifer heterogeneity on contaminant transport at the Hanford Site, *Ground Water*, *28*(6), 900–909.

R Development Core Team (2010), *R: A Language and Environment for Statistical Computing*, R Found. for Stat. Comput., Vienna.

Reading, H. G., and B. K. Lovell (1996), Controls on the sedimentary rock record, in *Sedimentary Environments: Processes, Facies, and Stratigraphy*, edited by H. G. Reading, pp. 5–37, Blackwell Sci., Cambridge, Mass.

Rubin, Y., and S. S. Hubbard (2005), *Hydrogeophysics*, 523 pp., Springer, New York.

Sangree, J. B., and J. M. Widmier (1979), Interpretation of depositional facies from seismic data, *Geophysics*, *44*(2), 131–160.

Scheibe, T., Y. Fang, C. J. Murray, E. E. Roden, J. Chen, Y. Chien, S. C. Brooks, and S. S. Hubbard (2006), Transport and biogeochemical reactions of metals in a physically and chemically heterogeneous aquifer, *Geosphere*, *2*(4), 220–235, doi:10.1130/GES00029.1.

Seaman, J. C., T. Murphy, and S. Walling (2009), Clay mineralogy of sediment cores collected from the EM-32 applied field research site, report, Savannah River Ecol. Lab., Aiken, S. C.

Seeboonruang, U., and T. R. Ginn (2006a), Upscaling heterogeneity in aquifer reactivity via the exposure-time concept: Inverse model, *J. Contam. Hydrol.*, *84*, 155–177.

Seeboonruang, U., and T. R. Ginn (2006b), Upscaling heterogeneity in aquifer reactivity via the exposure-time concept: Forward model, *J. Contam. Hydrol.*, *84*, 127–154.

Serkiz, S. M., W. H. Johnson, and L. M. J. Wile (2007), Environmental availability of uranium in an acidic plume at the Savannah River Site, *Vadose Zone J.*, *6*(2), 354–362.

Sherman, D. M., C. L. Peacock, and C. G. Hubbard (2008) Surface complexation of U(VI) on goethite (alpha-FeOOH), *Geochim. Cosmochim. Acta*, *72*(2), 298–310.

Slater, L. (2007), Near surface electrical characterization of hydraulic conductivity: From petrophysical properties to aquifer geometries—A review, *Surv. Geophys*, *28*, 169–197.

Smits, A. D., M. K. Harris, K. L. Hawkins, and G. P. Flach (1997), Integrated hydrogeological model of the general separations area (U), Re. *WSRC-TR-96-0399*, Savannah River Lab., Aiken S. C.

Spycher, N., S. Mukhopadhyay, D. Sassen, H. Murakami, S. Hubbard, J. Davis, and M. Denham (2011), On modeling H+ and U transport behavior in an acidic plume, *Mineral. Mag.*, *75*(3), 1925.

Strom, R. N., and D. S. Kaback (1992), SRP baseline hydrogeologic investigation: Aquifer characterization, groundwater geochemistry of the Savannah River Site and vicinity, *Rep. WSRC-RP–92-450 (DE93 003187)*, Environ. Sci. Sect., Savannah River Lab., Westinghouse Savannah River Co., Aiken, S. C.

Tidwell, V. C., A. L. Gutjahr, and J. L. Wilson (1999), What does an instrument measure? Empirical spatial weighting functions calculated from permeability data sets measured on multiple sample supports, *Water Resour. Res.*, *35*(1), 43–54.

Tronicke, J., K. Holliger, W. Barrash, and M. D. Knoll (2004), Multivariate analysis of cross-hole georadar velocity and attenuation tomograms for aquifer zonation, *Water Resour. Res.*, *40*, W01519, doi:10.1029/2003WR002031.

van Helvoort, P.-J., P. Filzmoser, and P. F. M. van Gaans (2005), Sequential factor analysis as a new approach to multivariate analysis of heterogeneous geochemical datasets: An application to a bulk chemical characterization of fluvial deposits (Rhine–Meuse delta, the Netherlands), *Appl. Geochem.*, *20*, 2233–2251.

van Overmeeren, R. A. (1998), Radar facies of unconsolidated sediments in the Netherlands: A radar stratigraphy interpretation method for hydrogeology, *J. Appl. Geophys.*, *40*, 1–18.

Vereecken, H., A. Binley, G. Cassiani, A. Revil, and K. Titov (2006), Applied Hydrogeophysics, NATO Sci. Ser., Ser. IV, *Earth Environ. Sci.*, vol. 71, Springer, Dordrecht, Netherlands.

Wan, J., T. K. Tokunaga, W. Dong, M. E. Denham, and S. S. Hubbard (2012), Persistent source influences on the trailing edge of a groundwater plume, and natural attenuation timeframes: The F-Area Savannah River site, *Environ. Sci. Technol.*, *46*(8), 4490–4497.

Xu, T., N. Spycher, E. Sonnenthal, G. Zhang, L. Zheng, and K. Pruess (2011), TOUGHREACT version 2.0: A simulator for subsurface reactive transport under non-isothermal multiphase flow conditions, *Comput. Geosci.*, *37*, 763–774.

Zappa, G., R. Bersezio, F. Felletti, and M. Giudici (2006), Modeling heterogeneity of gravel-sand, braided stream, alluvial aquifers at the facies scale, *J. Hydrol.*, *325*, 134–153.

DISCLAIMER

This document was prepared as an account of work sponsored by the United States Government. While this document is believed to contain correct information, neither the United States Government nor any agency thereof, nor The Regents of the University of California, nor any of their employees, makes any warranty, express or implied, or assumes any legal responsibility for the accuracy, completeness, or usefulness of any information, apparatus, product, or process disclosed, or represents that its use would not infringe privately owned rights. Reference herein to any specific commercial product, process, or service by its trade name, trademark, manufacturer, or otherwise, does not necessarily constitute or imply its endorsement, recommendation, or favoring by the United States Government or any agency thereof, or The Regents of the University of California. The views and opinions of authors expressed herein do not necessarily state or reflect those of the United States Government or any agency thereof or The Regents of the University of California.

Ernest Orlando Lawrence Berkeley National Laboratory is an equal opportunity employer.